Politecnico di Torino

Department of Environment, Land and Infrastructure Engineering

Master of Science in Georesources and Geoenergy Engineering

Static and dynamic model of a real hydrocarbon reservoir for future conversion to underground CO2 sequestration.

Supervisors:

Prof. Vera Rocca

Prof. Christoforos Benetatos

Candidate:

Jundi Ahmad (s313459)

Abstract

Addressing the escalating challenges of climate change necessitates a concerted effort to curtail atmospheric CO_2 levels, positioning carbon capture, utilization, and storage (CCUS) technologies as pivotal strategies. Among these, geological sequestration in depleted hydrocarbon reservoirs, coupled with adjacent aquifers, presents a promising media for carbon storage. This thesis examines the technical viability of repurposing the Norne Field, an oil and gas reservoir situated in the Norwegian Sea, for large-scale underground CO_2 sequestration. A detailed static reservoir model was put together, using data from the Open Porous Media (OPM) [46] initiative, and subsequently visualized using FloViz. This model explains the reservoir's complex geological structure, delineating its compartmentalization into distinct segments (C, D, E, and G) and characterizing key petrophysical attributes, notably an average porosity of 25% and a permeability of 900 mD. By using ECLIPSE® 100 of Schlumberger, dynamic simulations were conducted to evaluate the efficacy of three distinct CO_2 injection scenarios over a 15-year span (2019-2034), emphasizing injection into the existing gas cap by using pre-existing well infrastructure to avoid additional costs, and mainly focusing on physical and residual trapping mechanisms. The base case scenario, involving CO_2 injection through a single well at a rate of 2 million sm^3/day, resulted in a cumulative CO_2 injection of 20.38 million tons but exhibited suboptimal distribution within the gas cap, not using the full potential of the reservoir for storage. On one hand, Case 1, predicated on distributing the injection across eight wells at a reduced rate of 4 million sm^3/day over 8 wells, achieved a more substantial CO_2 injection of 40.76 million tons, moderately balancing storage capacity with robust pressure management. On the other hand, Case 2, which entailed injecting CO_2 through eight wells at an elevated rate of 6 million Sm^3/day over 8 wells, maximized CO_2 injection to 61.14 million tons

maintaining pressure thresholds. Comparative analysis of field pressure response (FPR), CO_2 saturation, and storage efficiency discloses that Case 2 as the optimal approach, by matching the storage efficiency with the imperative of preserving reservoir integrity and stability. Due to the data availability in ECLIPSE® 100 of Schlumberger format, this study was performed on injecting CO_2 as a solvent. Future research endeavors should prioritize the implementation of compositional simulators for detailed phase behavior and geochemical interaction analysis. This research supports CCUS viability in real hydrocarbon reservoirs for sustainable energy practices.

Dedications

As I reach the end of this long and challenging journey, I find myself overwhelmed with gratitude for the incredible support I have received. First and foremost, my deepest love and appreciation go to my family, my dearest friends and to the people I met during this journey that became family. You have been my constant anchors, offering unwavering encouragement and understanding when I needed it most. Your belief in me, even when my own faltered, has been the driving force behind this accomplishment. Thank you for celebrating every small victory and for helping me navigate the inevitable setbacks with grace and resilience. I am eternally grateful for your presence in my life.

I am also profoundly grateful to my supervisors, Prof. Vera Rocca and Prof. Christoforos Benetatos, for their guidance, mentorship, and patience. Your expertise and insightful feedback have been invaluable in shaping this thesis, and I am deeply appreciative of the time and effort you dedicated to my development, and thankful for your encouragement, which motivated me to push the boundaries of my knowledge.

I extend my sincere thanks to Politecnico di Torino for providing a stimulating academic environment and the resources necessary to pursue this research. The knowledge, skills, and experiences I have gained during my time here will undoubtedly serve as a strong foundation for my future endeavors.

Contents

Scope of Work

This thesis investigates the potential of the depleted Norne Field in the Norwegian Sea for large-scale CO_2 storage to mitigate climate change. A multidisciplinary approach was used, integrating geological data and fluid flow simulation.

The work encompassed:

- **Static Model Refinement:** Review and refinement of the existing static reservoir model from the Open Porous Media (OPM) initiative, representing the field's compartmentalized structure (segments C, D, E, and G) and petrophysical properties (average porosity of 25% and permeability of 900 mD).
- **Dynamic Simulation:** ECLIPSE® 100 ("black oil model") simulations focused on structural, stratigraphic, and residual trapping, aligning with the study's timeframe and data availability. Three CO_2 injection scenarios over 15 years (2019-2034) were evaluated using existing wells and infrastructure.
- **Comparative Analysis:** Comparison of field pressure response, CO_2 saturation, and storage efficiency to determine the optimal injection strategy.
- **Results and Discussion:** Analysis of results, showing that injecting CO_2 through eight wells at 6 million Sm3/day (Case 2) maximized CO_2 injection while preserving reservoir integrity and stability.

This research contributes to understanding CCUS viability and provides a basis for future research with compositional simulators for detailed phase behavior and geochemical interaction analysis.

I.Introduction

One of the most serious challenges of the 21st century is mitigating the impact of climate change, primarily driven by the accumulation of greenhouse gases in the atmosphere. Carbon Dioxide (CO_2) is the most significant anthropogenic greenhouse gas, and its accumulation is largely attributed to human activities such as the burning of fossil fuels in energy production and industrial processes. The increase in atmospheric CO_2 has intensified global warming and contributed to associated environmental changes, from rising sea levels to ecosystem disruptions [1]. To decrease these detrimental effects, significant reductions in CO_2 emissions are necessary, and carbon capture, utilization, and storage (CCUS) technologies require a critical approach to cut down atmospheric CO_2 levels [2].

Carbon Dioxide (CO_2) capture is important in sectors where emissions are difficult to reduce, such as energy production, cement, and steel manufacturing [3]. Several methods have been developed for capturing CO_2, including pre-combustion capture, post-combustion capture, and oxy-fuel combustion, each of which involves separating CO_2 from the waste gases produced by fossil fuel combustion or other industrial processes [1]. Direct air capture (DAC), which extracts CO_2 directly from the atmosphere, and biological capture methods, such as Bioenergy with Carbon Capture and Storage (BECCS), where CO_2 is absorbed by plants and then captured during bioenergy processes, are also emerging as critical technologies [4].

Once CO_2 is captured, it must be safely stored or employed to make sure it does not return to the atmosphere. Geological storage in depleted reservoirs and deep saline aquifers are the most promising long-term solutions [5]. Depleted gas reservoirs with associated aquifers are particularly attractive for CO_2 storage because they have proven their ability to trap gas over geological timescales and because aquifers can help maintain pressure during injection [6].

Aquifers play a crucial role in maintaining pressure during injection processes. When water or other fluids are injected into an aquifer, the pressure within the aquifer increases, which helps sustain hydraulic equilibrium and prevents excessive depletion of underground resources. This is specifically useful in confined aquifers, where the injected fluid creates overpressure that can counteract subsidence or stabilize the surrounding geological structures. CO_2 storage in these geological formations involves injecting the gas underground, where it becomes trapped in porous rock layers beneath an impermeable caprock. Several mechanisms contribute to its long-term immobilization, including physical trapping, dissolution into formation water, and mineralization, where CO_2 reacts with surrounding rock to form stable minerals [7]. These processes ensure that CO_2 remains sequestered over long periods, reducing the risk of leakage back to the surface.

Injecting CO_2 into depleted reservoirs not only provides a secure storage option but also offers the potential to enhance hydrocarbon recovery by increasing reservoir pressure. The injected CO_2 reduces oil viscosity and improves overall fluid mobility, allowing for better oil displacement and recovery. Furthermore, CO_2 injection can lead to oil swelling, which increases the oil volume and improves its mobility, making it easier to extract from the reservoir. This dual benefit makes it an appealing strategy for CO_2 management during the energy transition [8]. The following sections will explore the specific mechanisms, challenges, and opportunities associated with CO_2 injection into such reservoirs, particularly focusing on the role of aquifers in maintaining pressure and enhancing the security of CO_2 storage.

II. Overview of Underground Carbon Dioxide Storage

1. Main Factors Affecting CO_2 Storage

a. Mechanisms of CO_2 Storage

The effectiveness of underground CO_2 storage relies on several trapping mechanisms that operate over different timescales, as shown in the figure 1 (Fig.1).

Structural Trapping

It is the most immediate mechanism, where CO_2 is physically trapped under impermeable caprock layers that act as barriers to upward migration. It is the initial mechanism that comes into play when CO_2 is injected into a reservoir. It occurs when the buoyant CO_2 plume is physically trapped beneath impermeable layers of rock, known as caprock. The caprock acts as a seal, preventing the upward migration of CO_2. Typically, structural traps are formed by geological features such as anticlines, faults, or stratigraphic variations that confine CO_2 to specific parts of the reservoir. In many cases, structural trapping is the primary method of containment in the early stages of CO_2 injection. However, the security of this mechanism depends heavily on the integrity of the caprock. Over time, structural trapping provides the necessary conditions for additional trapping mechanisms to take effect, further stabilizing the stored CO_2 [15].

Residual Trapping

It occurs when CO_2 becomes immobilized in pore spaces due to capillary forces, providing additional containment security. CO_2 is pushed through the porous rock formations by the movement of formation water or brine. During this process, small droplets or bubbles of CO_2

become trapped in the pore spaces of the rock due to capillary forces. This is sometimes referred to as capillary trapping, and it is essential in immobilizing CO_2. Once the CO_2 becomes residually trapped, it is unable to move further, even in the presence of pressure gradients within the reservoir. This form of trapping is considered stable and can hold a significant portion of the injected CO_2 over long periods [16]. The effectiveness of residual trapping is affected by the porosity and permeability of the reservoir rock, as well as the wettability of the rock surface.

Solubility Trapping

Over time, it becomes significant as CO_2 dissolves in the formation water, reducing its buoyancy and risk of leakage. Solubility trapping involves the dissolution of CO_2 into formation water (brine) over time. When CO_2 dissolves in water, it forms carbonic acid (H_2CO_3), which dissociates into bicarbonate (HCO_3^-) and carbonate (CO_3^{2-}) ions. This process significantly reduces the mobility of CO_2, as the gas becomes part of the liquid phase, preventing it from escaping or migrating within the reservoir. The solubility of CO_2 in water increases with pressure and decreases with temperature, making deeper, cooler reservoirs more suitable for solubility trapping [7]. Over time, the dissolved CO_2 can react with minerals in the reservoir rock, leading to further immobilization through mineral trapping. Solubility trapping is a particularly effective mechanism for enhancing long-term storage security, as dissolved CO_2 is less likely to leak compared to free-phase CO_2 [15].

Here's the list of equations that take place in solubility trapping:

1.Dissolution of CO_2 in Water:

$$CO_2\ (g) \Leftrightarrow CO_2\ (aq)$$

2.Formation of Carbonic Acid:

$$CO_2\ (aq) + H_2O\ \Leftrightarrow H_2CO_3$$

3.Dissociation of Carbonic Acid:

$$H_2CO_3 \Leftrightarrow H^+ + HCO_3^-$$

4. Further Dissociation to Carbonate Ions:

$$HCO_3^- \Leftrightarrow H^+ + CO_3^{2-}$$

Mineral Trapping

It is the most permanent mechanism, wherein dissolved CO_2 reacts with minerals in the reservoir rock to form stable carbonate precipitates. Each of these mechanisms contributes to the overall safety and permanence of CO_2 storage. Mineral trapping is the most secure and permanent form of CO_2 sequestration. It occurs when dissolved CO_2 reacts with minerals in the surrounding rock to form stable carbonate minerals, such as calcite ($CaCO_3$), dolomite ($CaMg(CO_3)_2$), or siderite ($FeCO_3$). These reactions take place over long timescales, often requiring decades to centuries to convert significant amounts of CO_2 into solid carbonates. While slow, mineral trapping is considered the most reliable form of CO_2 storage because the CO_2 is converted into a solid form that is highly unlikely to migrate or escape from the reservoir. The extent of mineral trapping depends on several factors, including the availability of reactive minerals such as silicates or carbonates, the temperature and pressure of the reservoir, and the chemical composition of the formation water [18]. Mineral trapping can also affect the physical properties of the reservoir. As carbonate minerals precipitate, they may clog pore spaces,

reducing permeability. However, in some cases, this precipitation may also enhance the mechanical strength of the reservoir, further securing the stored CO_2 [9][10] [17].

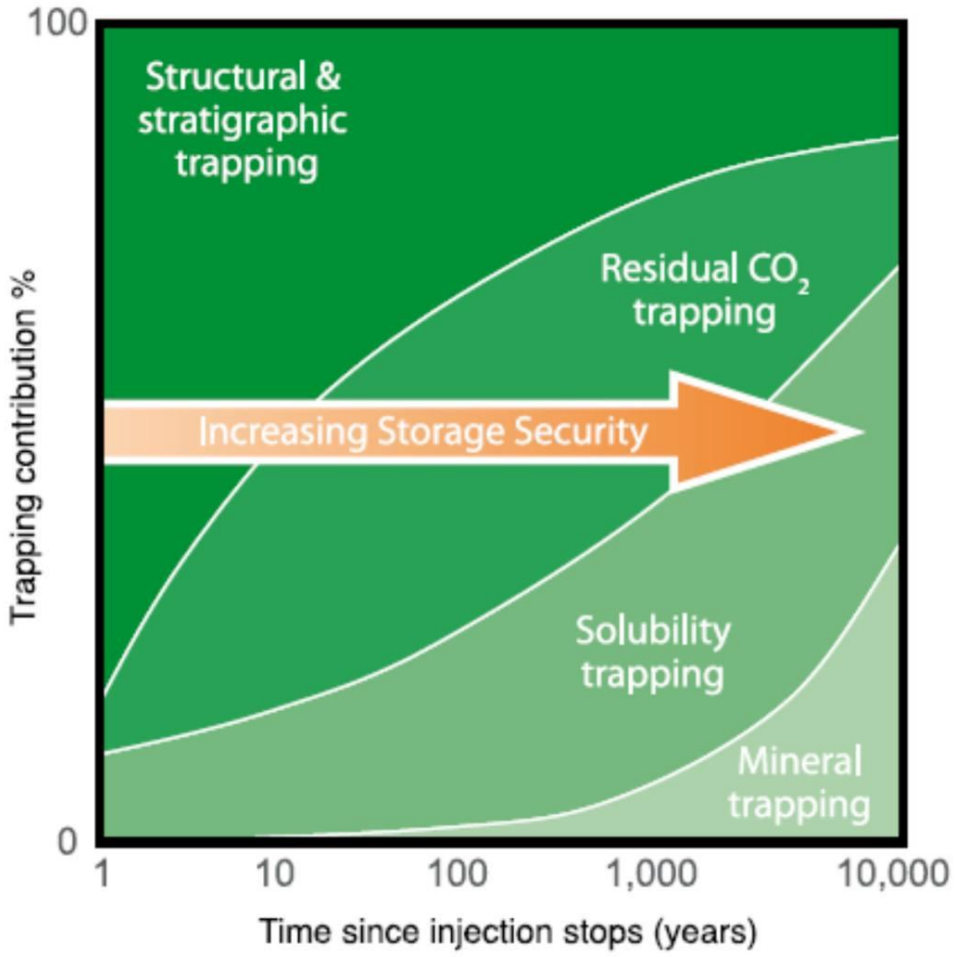

Figure 1:Contribution of CO_2 Trapping Mechanisms Over Time and Their Impact on Storage Security [14]

b. *Types of Geological Storage Formations*

Numerous types of geological formations are convenient for CO_2 storage, each represent individual benefits and challenges. Saline aquifers are one of the most promising choices due to their widespread availability and huge storage capacity. These formations contain brine unsuitable for human application, making them ideal for sequestration purposes [7]. Depleted reservoirs are another viable option, offering pre-existing infrastructure and proven containment through their history of hydrocarbon storage. Moreover, unmineable coal seams can adsorb CO_2 onto coal surfaces while displacing methane gas; however, their limited permeability poses operational challenges [11]. Emerging options such as basaltic formations show potential for rapid mineralization but need additional research to tackle technological and economic barriers.

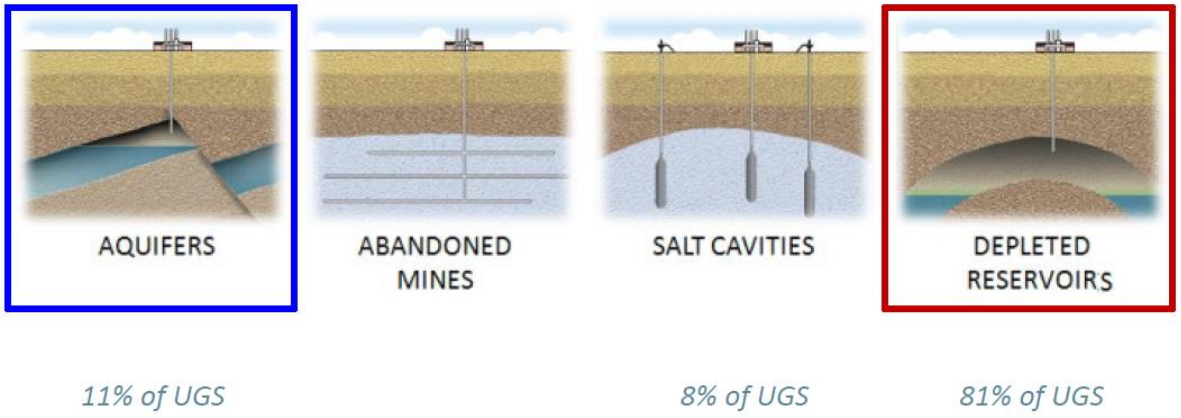

Figure 2: Types of Underground Gas Storage (UGS) Facilities and Their Global Distribution

c. *Criteria for Suitable Storage Sites*

The selection of a suitable site for underground CO_2 storage is chosen based on several geological and operational factors. Depth is a critical factor because CO_2 must be injected at depths greater than 800 meters to ensure it remains in a supercritical state, where its density

increases, and its storage volume decreases [13]. Additionally, permeability is essential for the ease of flow of CO_2 where it should be higher than 100 mD. Caprock integrity is also critical since it prevents leakage of CO_2 when it is impermeable (<0.1 mD) and capable of enduring injection-induced pressure changes. Other factors include reservoir porosity, which determine injectivity and storage capacity, as well as the presence of faults or fractures that could cooperate the containment. Furthermore, the viscosity of CO_2 at reservoir conditions significantly impacts injectivity, with lower viscosity generally leading to higher injectivity and improved storage efficiency [9].

d. Monitoring and Verification.

Monitoring technologies are needed for ensuring the safety and effectiveness of underground storage projects. Seismic surveys are frequently used to track the migration of injected CO_2 plumes within the subsurface. Pressure monitoring helps detect potential risks such as overpressure or caprock failure. Moreover, tracer studies can recognize leakage pathways if they take place [10]. Advanced techniques like satellite-based InSAR (Interferometric Synthetic Aperture Radar) present ground deformation data that reveals subsurface changes related to injection activities [13]. Effective monitoring not only confirms compliance with regulatory standards but also builds public confidence in CCS technology.

e. Challenges and Risks

Regardless of its potential, underground CO_2 storage encounters several challenges that must be faced to ensure its feasibility at scale. Leakage risks remain a primary worry, particularly through abandoned wells or faults that may serve as conduits for upward migration [11]. Injection-induced seismicity is another issue that can arise from pressure changes within the reservoir. Furthermore, chemical interactions between CO_2-saturated brine and reservoir rocks

can alter porosity and permeability over time, potentially affecting storage capacity [9]. Addressing these challenges requires strong site selection processes, advanced modeling techniques, and continuous monitoring.

2. Pressure-Volume-Temperature CO_2 Behavior

For an effective underground carbon dioxide (CO_2) geological storage, it is fundamental to understand the chemical and thermodynamic conditions governing its behavior. CO_2 transitions between solid, liquid, gas, and supercritical states is contingent on specific temperature and pressure conditions, as illustrated by its phase diagram below (fig. 3).

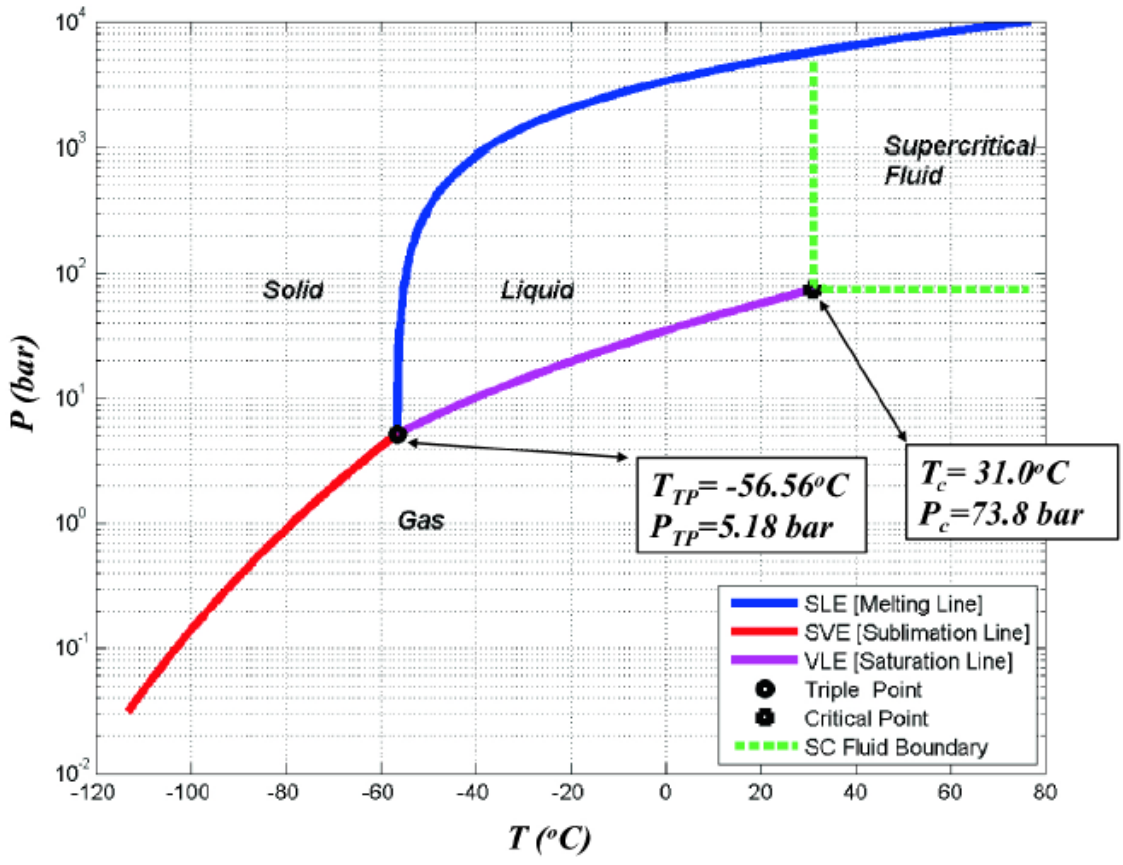

Figure 3: Phase diagram P vs T of CO_2

The phase diagram of CO_2 offers a detailed description of its physical states under various temperature and pressure combinations. The triple point of CO_2 occurs at -56.56°C and 5.18 bar, where solid, liquid, and gas phases coexist in equilibrium. Below this pressure, liquid CO_2 cannot exist; instead, solid CO_2 sublimates directly into gas, which is why solid CO_2 (dry ice) transitions directly to vapor at standard atmospheric pressure without forming a liquid phase. At the critical point (31.0°C and 73.8 bar), the distinction between liquid and gas phases vanishes. Beyond this point, CO_2 enters a supercritical state where it shows properties of both liquids and gases—expanding like a gas but with densities like liquids. This supercritical state is important for carbon capture and storage (CCS) applications because it allows CO_2 to be stored efficiently in underground formations due to its high density and low viscosity. The phase behavior of CO_2 is highly sensitive near the critical point. Small changes in temperature or pressure around this area can result in significant changes in density, viscosity, compressibility factor "z" and gas formation factor "Bg" thermodynamic properties. For example:

- Below the critical temperature, increasing pressure results in rapid density increases as CO_2 transitions from a gaseous to a liquid-like state.
- Above the critical temperature, density changes become linear with pressure increases, characteristic of supercritical fluids.[19][20][21]

a. Density

The behavior of carbon dioxide (CO_2) near its critical point (31.1°C, 73.8 bar) is distinguished by remarkable transformations in density as pressure increases. These changes are mainly due to the thermodynamic properties of CO_2, particularly its compressibility and phase transition behavior. The figure (fig.4) below shows the variation of density of CO_2 in different temperatures and pressures ranges.

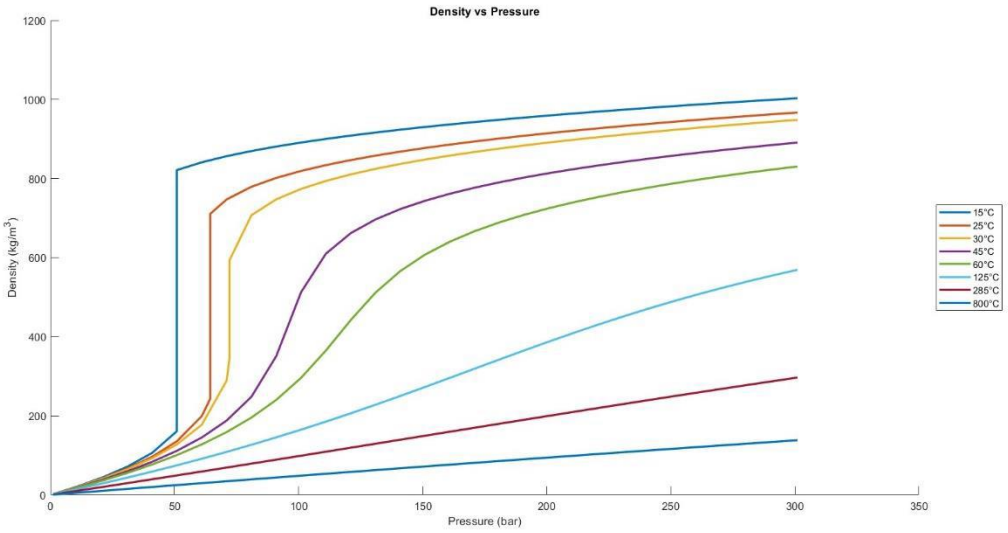

Figure 4: The variation of density of CO_2 in different temperatures and pressures ranges

Density Behavior Near the Critical Point

At the critical point, CO_2 exists in a supercritical state where it exhibits properties of both gases and liquids. The density of CO_2 near this point is extremely sensitive to small changes in pressure and temperature. At the critical temperature (31.1°C) and critical pressure (73.8 bar), liquid and vapor phases coexist with the same density, approximately 467.6 kg/m³.

This phenomenon marks the disappearance of a distinct liquid-vapor boundary.

Below the Critical Temperature

When CO_2 is just below its critical temperature but near its critical pressure, small increases in pressure cause rapid increases in density. This behavior reflects the high compressibility of CO_2 in this region, as intermolecular forces become increasingly significant. For example, at pressures slightly above 73.8 bar and temperatures below 31.1°C, CO_2 transitions from a gaseous to a liquid-like state, resulting in a steep rise in density.

Above the Critical Temperature

Once CO_2 surpasses its critical temperature, it enters a supercritical phase where it no longer exhibits a clear phase transition between gas and liquid. In this state:

- The density increase with pressure becomes steadier and more linear compared to the sharp rise observed below the critical temperature.
- Supercritical CO_2 maintains relatively high densities (e.g., 300–800 kg/m³ depending on pressure), but these densities are lower than those of liquids at standard conditions.

Thermodynamic Properties Influencing Density

The steep variations in density near the critical point are attributed to the unique thermodynamic properties of CO_2:

1. Compressibility: The compressibility factor (z) of CO_2 deviates significantly from unity near the critical point due to strong intermolecular forces. Below the critical temperature, attractive forces dominate, causing z to be less than one and leading to higher densities.
2. Phase Transition Dynamics: Near-critical fluids exhibit large fluctuations in density due to their sensitivity to pressure and temperature changes. These fluctuations diminish as pressure increases further above the critical point.

Density of Higher Pressures

As pressure increases well beyond the critical point (e.g., >100 bar), the rate of density change becomes smoother and less pronounced:

- For pressures between 75–11bar at temperatures slightly above 31°C, CO_2 density can range from approximately 300 to 700 kg/m³.
- At pressures exceeding 100 bar, further increases result in smaller density variations because intermolecular repulsion dominates over attractive forces.

This behavior makes supercritical CO_2 particularly useful for industrial applications like carbon capture and storage (CCS) or enhanced oil recovery (EOR). Its high density allows for efficient storage, while its gas-like diffusivity facilitates injection into reservoirs. [22][23]

b. Viscosity

The viscosity of carbon dioxide (CO_2) is a critical property that influences its flow and transport in various applications, including carbon capture and storage (CCS), enhanced oil recovery (EOR), and supercritical fluid processes. Like its density, the viscosity of CO_2 is highly dependent on temperature, pressure, and phase state (gas, liquid, or supercritical). Below is an in-depth exploration of how CO_2 viscosity behaves under different conditions. The graph below (Fig.5) shows the variation of viscosity of CO_2 in different temperatures and pressures ranges.

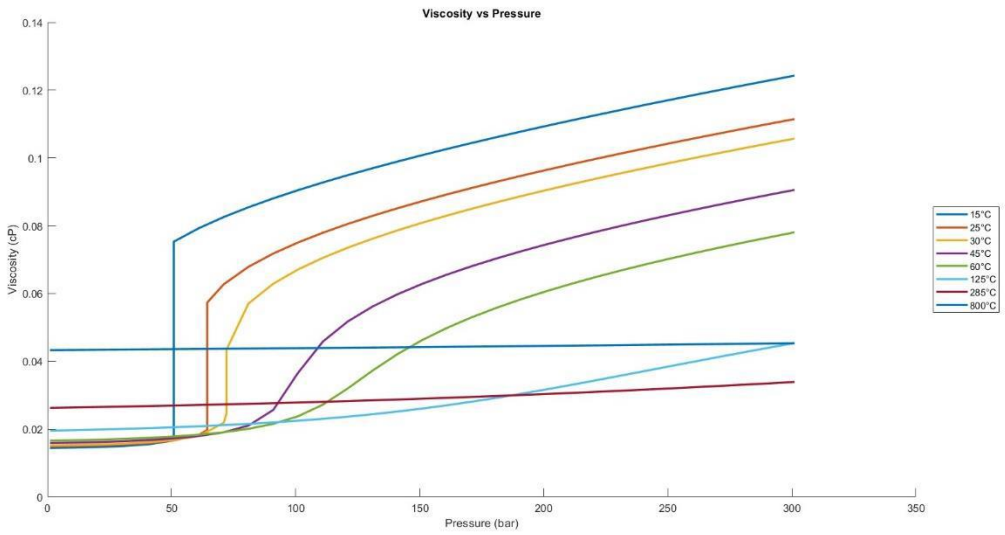

Figure 5: The variation of viscosity of CO_2 in different temperatures and pressures ranges.

Viscosity in the Gaseous State

In its gaseous phase, CO_2 has relatively low viscosity compared to liquids. The viscosity of gaseous CO_2 increases with temperature because higher temperatures lead to greater molecular kinetic energy, which enhances momentum transfer between molecules. However, at low pressures, the viscosity remains nearly independent of pressure due to the weak intermolecular forces in the gaseous state.

Viscosity Near the Critical Point

The behavior of CO_2 viscosity becomes more complex near its critical point. In this range:

- **Critical Enhancement**: The viscosity exhibits a sharp increase due to the critical enhancement effect, where intermolecular interactions become stronger as the gas transitions toward a liquid-like state. This phenomenon occurs within a narrow range around the critical point.

- **Density Dependence**: Viscosity becomes highly sensitive to density changes near the critical point. As density increases with pressure, the viscosity rises sharply.

Viscosity in the Liquid State

In its liquid phase (below the critical temperature but at high pressures), CO_2 exhibits higher viscosities compared to its gaseous or supercritical states:

- Viscosity increases linearly with pressure along isotherms due to stronger intermolecular forces.
- However, it decreases with increasing temperature because higher thermal energy reduces molecular interaction strength.

Factors Influencing Viscosity

Several factors influence CO_2 viscosity across its phases:

1. **Temperature**: Viscosity generally decreases with increasing temperature across all phases due to reduced intermolecular forces at higher thermal energy levels.
2. **Pressure**: In gaseous and supercritical states, viscosity increases with pressure due to increased density and molecular interactions.
3. **Phase Transitions**: Near phase boundaries (e.g., gas-liquid or gas-supercritical), sharp changes in density lead to significant variations in viscosity.[21][25][26]

c. Compressibility Factor z

The compressibility factor (z) of carbon dioxide (CO_2) displays significant variations as it approaches and surpasses its critical point (31.1°C, 73.8 bar). “Z” is a measure of how much a real gas deviates from ideal gas behavior, where Z=1 represents ideal behavior. For CO_2, the

behavior of z across different pressures and temperatures highlights its non-ideal nature near the critical point and its transition between gas-like and liquid-like states. The graph below (Fig.6) showcases the variation of the compressibility factor z of CO_2 in different temperatures and pressures ranges.

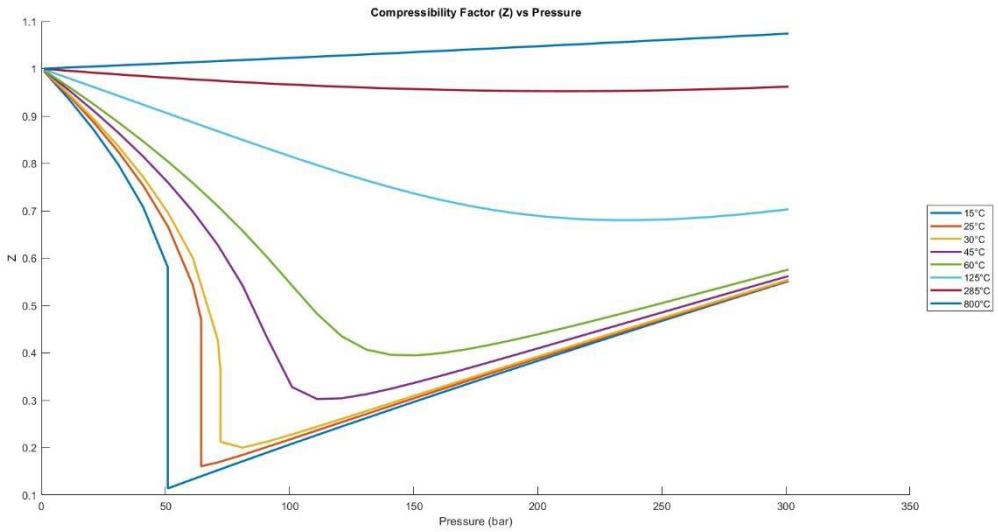

Figure 6: The variation of the compressibility factor z of CO_2 in different temperatures and pressures ranges

Below the Critical Pressure

At pressures below the critical point (73.8 bar), z decreases sharply as CO_2 approaches its critical temperature (31.1°C). This decrease is particularly pronounced at temperatures below the critical temperature, where CO_2 behaves as a gas but exhibits strong intermolecular attractions. These attractions cause deviations from ideal gas behavior, resulting in Z<1. This indicates that CO_2 is more compressible than an ideal gas under these conditions.

Near the Critical Point

Close to the critical point (31.1°C and 73.8 bar), z exhibits a pronounced dip due to the transition from gas-like to liquid-like behavior. This region is characterized by:

- Critical Enhancement: Near the critical point, small changes in pressure or temperature led to large density fluctuations, causing significant deviations in z.
- Phase Transition: The dip in z reflects the coexistence of gas-like and liquid-like properties as CO_2 transitions into a supercritical fluid. The compressibility factor becomes highly sensitive to minor changes in thermodynamic conditions during this phase.

This behavior is crucial for applications like carbon capture and storage (CCS), as it affects how CO_2 can be compressed and transported efficiently.

Above the Critical Temperature

Once CO_2 surpasses its critical temperature (31.1°C), it enters a supercritical state where it no longer exhibits distinct liquid or gas phases. In this region:

- At higher pressures, z approaches value closer to 1, indicating more ideal gas-like behavior.
- The intermolecular forces are less dominant compared to near-critical conditions, leading to smoother changes in compressibility with increasing pressure.[26][28][29]

d. Gas Formation Factor Bg

The Gas Formation Volume Factor (Bg) is an important parameter in reservoir engineering that illustrates the relationship between the volume of gas at reservoir conditions (pressure and temperature) and its volume at standard surface conditions. It is a dimensionless ratio that

provides insights into how gas expands or compresses as it transitions between these two states. As shows the graph (Fig.7) below, Bg decreases rapidly with increasing pressure, particularly near the critical pressure of 73.8 bar. Below the critical temperature of 31.1°C, Bg shows more obvious changes as CO_2 compresses. Above the critical temperature, the decrease in Bg stabilizes more quickly, indicating the behavior of supercritical CO_2, where the volume becomes less sensitive to temperature changes.

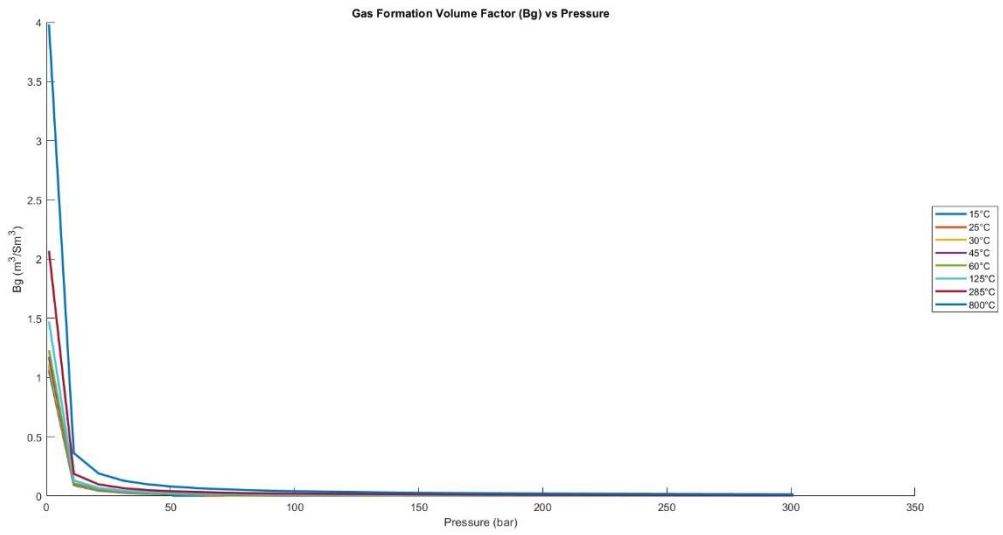

Figure 7: The variation of the compressibility factor z of CO_2 in different temperatures and pressures ranges.

3. Rock-Fluid Properties

a. Capillary Pressure

Capillary pressure is a critical parameter in CO_2 storage as it governs the distribution and movement of CO_2 and brine within the pore spaces of the reservoir rock. It is defined as the

pressure difference across the interface of two immiscible fluids (e.g., CO_2 and brine) and is influenced by factors such as interfacial tension, wettability, and pore throat size. Capillary pressure plays a key role in determining the height of the CO_2 column that can be trapped beneath a sealing caprock, which directly impacts the structural trapping efficiency. For instance, higher capillary entry pressures in fine-grained rocks, such as shales or mudstones, act as barriers to CO_2 migration, enhancing containment security. However, variations in pore throat size and heterogeneities in capillary pressure across the reservoir can lead to uneven plume migration during injection, potentially reducing storage efficiency [30]. Moreover, capillary pressure is highly sensitive to reservoir conditions such as temperature, pressure, and brine salinity. For example, increased reservoir pressure reduces interfacial tension between CO_2 and brine, subsequently lowering capillary entry pressure. This can enhance injectivity but may also reduce the effectiveness of structural trapping. Conversely, higher salinity increases interfacial tension, raises capillary entry pressures and improves containment potential [36]. Additionally, geochemical interactions between injected CO_2 and rock minerals can alter pore structure over time. For instance, mineral dissolution may increase pore throat size and reduce capillary pressures locally, while precipitation may have the opposite effect [37]. Capillary pressure also affects residual trapping mechanisms by immobilizing a portion of CO_2 within pore spaces due to capillary forces. This is particularly significant in heterogeneous reservoirs where regions with smaller pores exhibit higher residual saturations. Advanced modeling techniques such as lattice Boltzmann simulations have been used to study these effects at the pore scale, providing insights into how capillary forces influence CO_2 migration and storage efficiency [37]. Overall, understanding and accurately modeling capillary pressure are essential for optimizing CO_2 injection strategies and ensuring long-term storage security.

b. *Wettability*

Wettability is a crucial factor in CO_2 storage, as it determines the interaction between reservoir rock surfaces, brine, and CO_2, influencing capillary pressure, relative permeability, and trapping mechanisms. In water-wet systems, CO_2 is more effectively trapped in pore spaces due to capillary forces, enhancing residual trapping. However, under high-pressure and high-temperature conditions typical of reservoirs, wettability can shift toward intermediate or CO_2-wet states, especially in carbonate rocks like calcite. This shift reduces capillary trapping but enhances injectivity. Factors such as mineral composition, brine salinity, and CO_2 impurities (e.g., N_2) significantly affect wettability. For instance, impurities can enhance water-wettability at specific concentrations, improving storage security. Understanding wettability behavior is essential for optimizing injection strategies and ensuring long-term containment [42][43].

c. *Interfacial Tension*

Interfacial tension (IFT) between CO_2 and brine is a key parameter influencing capillary pressure, CO_2 plume migration and trapping mechanisms. IFT determines the capillary entry pressure required for CO_2 to displace brine in the reservoir rock. It is highly dependent on pressure, temperature, and salinity. Studies show that as pressure increases, IFT decreases, which enhances CO_2 mobility but may reduce capillary trapping efficiency. Similarly, higher salinity increases IFT, potentially reducing storage capacity. The mineral composition of the reservoir rock also affects IFT, as different minerals can alter the wettability and interfacial properties of the system. Advanced models, such as ensemble learning techniques, have been developed to predict IFT under various conditions, enabling better estimation of storage capacity and safety in reservoirs [30][31].

d. Contact Angle

The contact angle reflects the wettability of the rock surface and determines whether the reservoir is water-wet or CO_2-wet, but mostly the formations are water-wet. Wettability influences capillary trapping and flow behavior within the reservoir. Under high-pressure and high-temperature conditions typical of geological storage sites, contact angles may shift toward intermediate wettability, especially in carbonate rocks. This shift can reduce capillary trapping efficiency but enhance injectivity. Factors such as mineral composition, surface roughness, and brine salinity significantly affect contact angles. [32][33]

e. Relative Permeability

Relative permeability is a critical parameter in CO_2 storage, as it quantifies the ability of multiple fluids, such as CO_2 and brine, to flow simultaneously through porous rock. It is dependent on the saturation of each fluid and is influenced by factors such as wettability, interfacial tension (IFT), and pore structure. In CO_2-brine systems, relative permeability curves are essential for predicting injectivity, plume migration, and trapping mechanisms. For instance, during CO_2 injection (drainage), the relative permeability of CO_2 increases as its saturation rises, while the brine's permeability decreases. Conversely, during imbibition (brine re-entry), hysteresis effects can lead to residual trapping of CO_2 in the pore spaces, enhancing storage security [37][40].

The interplay of capillary, viscous, and buoyancy forces also affects relative permeability. For example, capillary forces dominate in fine-grained rocks with small pores, leading to lower relative permeability for CO_2. On the other hand, viscous forces are more significant in high-permeability reservoirs, enhancing CO_2 mobility. Additionally, IFT between CO_2 and brine directly influences relative permeability curves by altering fluid distribution within the pore

spaces. Experimental studies have shown that higher IFT results in steeper relative permeability curves for both fluids, while lower IFT improves flow continuity for CO_2 [41].

f. Diffusivity

Diffusivity is a critical parameter in rock-fluid interactions during CO_2 storage, as it governs the transport of dissolved CO_2 and other chemical species within the reservoir. It plays a key role in solubility trapping, where CO_2 dissolves into brine, and in diffusion-limited geochemical reactions with reservoir minerals. The rate of molecular diffusion affects how dissolved CO_2 reaches reactive surfaces, influencing processes such as mineral dissolution and precipitation. For instance, in carbonate reservoirs, the dissolution of calcite or dolomite due to CO_2-brine interactions can increase porosity and permeability locally, enhancing injectivity but potentially weakening the rock structure. Diffusivity also impacts the spatial distribution of chemical alterations; near-wellbore regions often experience convection-dominated transport leading to rapid dissolution, while far-field regions are governed by slower diffusion-dominated processes. Factors such as pore structure, temperature, pressure, and brine salinity significantly influence diffusivity. Smaller pore throats reduce effective diffusivity due to increased tortuosity, while higher temperatures and pressures enhance molecular diffusion. Additionally, high salinity reduces CO_2 solubility and diffusivity due to ionic interactions. These factors collectively determine the efficiency of trapping mechanisms and the long-term stability of CO_2 storage. Accurate modeling of diffusivity is essential for predicting changes in porosity and permeability over time and for ensuring reservoir integrity

g. CO_2 Reactions

When CO_2 is injected into geological formations, it undergoes a series of geochemical reactions with the formation water (brine) and rock minerals, significantly altering the

reservoir's physical and chemical properties. Initially, CO_2 dissolves in the brine to form carbonic acid (H_2CO_3), which lowers the pH of the solution, creating an acidic environment. This acidic brine reacts with carbonate and silicate minerals in the rock, leading to dissolution and precipitation processes. For example, minerals like calcite ($CaCO_3$) dissolve, releasing calcium ions into the brine, while secondary minerals such as siderite ($FeCO_3$) and magnesite ($MgCO_3$) may precipitate under favorable conditions. The Fe (iron) and Mg (magnesium) come from two sources: the dissolution of iron and magnesium-bearing minerals in rock formation, and the pre-existing ions dissolved in the formation water or brine. As the CO_2-induced acidic environment promotes mineral dissolution, it increases the concentration of Fe and Mg ions in the brine, which can then participate in the precipitation of secondary minerals like siderite and magnesite. These reactions can increase porosity and permeability locally due to dissolution but may also reduce them over time due to mineral precipitation near injection wells [44][45]. The impact of these reactions varies spatially within the reservoir. Near the injection well, dissolution dominates initially, enhancing flow pathways. Over time, precipitation of secondary minerals can clog pore spaces and reduce injectivity. In contrast, regions farther from the injection site are primarily affected by dissolution, maintaining higher porosity and permeability. These geochemical interactions are influenced by reservoir conditions such as temperature, pressure, and mineral composition. High temperatures accelerate reaction rates, while high pressures increase CO_2 solubility in the brine. Additionally, impurities in injected CO_2 (e.g., N_2, H_2S) can alter reaction kinetics and mineral trapping efficiency [45]. Overall, these reactions play a crucial role in determining the efficiency of trapping mechanisms—such as solubility trapping (dissolution of CO_2 into brine) and mineral trapping (precipitation of stable carbonates)—and influence the long-term stability of CO_2 storage sites.

III. Model characterization

1. Numerical Simulation and Modelling

Static modeling in numerical simulation plays a critical role in carbon capture and storage (CCS) projects, and software like Schlumberger's Petrel is widely used to construct detailed 3D geological models. These models integrate data from seismic surveys, well logs, and core samples to define the structural framework, lithology, facies distribution, and petrophysical properties such as porosity and permeability. Petrel enables geoscientists to create high-resolution static models that serve as the foundation for dynamic simulations, helping to evaluate storage capacity, assess caprock integrity, and identify suitable injection sites. By offering advanced tools for integrating static and dynamic parameters, Petrel enhances the accuracy of CCS site characterization and supports decision-making for long-term CO_2 storage strategies

In addition to its contribution in static models' creation, numerical modelling is also essential for simulating and predicting the physical, chemical, and geo-mechanical processes involved in storing CO_2 underground. Carbon storage projects encompass a variety of underground basins, each with distinct challenges for CO_2 storage. Additionally, multiple trapping mechanisms operate during these processes, each contributing to securely immobilizing CO_2 underground. However, the interplay and combined effects of these mechanisms significantly increase the complexity of CCS projects, requiring advanced simulations capable of addressing their simultaneous impacts. Assessing the individual contribution of each mechanism is also challenging since CO_2 trapping depends not only on the fluid-rock mineral properties of the reservoir or aquifer but also on the injection strategy.

Moreover, these trapping mechanisms are interdependent. To address these complexities, numerical simulation software tools are indispensable. Examples of such tools ECLIPSE, which is designed to simulate CO_2 behavior under varying reservoir conditions and injection strategies.

The Norne Field, located in the Norwegian Sea, is an offshore oil and gas reservoir with a rich dataset and well-characterized geological features, making it an ideal candidate for carbon capture and storage (CCS) project. The field consists of three distinct zones: oil, gas, and water, with historical production supported by water injection for enhanced oil recovery (EOR). The reservoir exhibits porosity values ranging from 20% to 30% and permeability between 20 to 2500 mD, depending on the specific formation layer. Reservoir pressure has been maintained through injection strategies, ensuring its suitability for further studies involving CO_2 injection. Past operations have included water-alternating-gas (WAG) injection, which combines CO_2 and water to enhance oil recovery while simultaneously storing CO_2. In my thesis, I will focus on simulating CO_2 injection into the Norne Field to evaluate its capacity for long-term carbon storage. This study will involve analyzing the behavior of injected CO_2 under reservoir conditions, assessing trapping mechanisms such as structural and residual trapping, and investigating the impacts on reservoir pressure and integrity.

2. Static Model

The Norne field is a significant oil and gas reservoir located in the Norwegian Sea, approximately 85 kilometers north of the Heidrun field. Discovered in 1992, it began production on November 6, 1997, marking a milestone in Northern Norway's oil development [47]. The field is situated in Jurassic sandstone formations, with oil primarily found in the Ile and Tofte formations and gas in the Garn formation, at a depth of about 2,500 meters below sea level. It

is a significant offshore oil and gas field known for its production and reservoir management studies. The field has been extensively studied for advanced reservoir optimization and improved oil recovery techniques.

Figure 8: Norne field location

The data used in this thesis was obtained from the Open Porous Media (OPM) initiative, an open-source platform that provides publicly available datasets for reservoir simulation and modeling. The dataset utilized in this study served as the basis for the static model, which was subsequently modified to better suit the objectives of this research. Specifically, simplifications were made to the original static model to streamline the analysis while retaining its essential geological and reservoir features. These modifications included simplifying the representation of faults and horizons to reduce complexity while preserving their key structural and stratigraphic characteristics.

a. Reservoir Characterization

The Norne Field reservoir is characterized by several key properties that define its geological and production potential. These parameters, shown in the table below (Table 2), highlight the Norne field's significant hydrocarbon resources and its production history.

Table 1: Norne Field Key Properties

Reservoir Key Properties	*Value*
Depth (m)	*2578-2802*
Thickness (m)	*224*
Mean Porosity (-)	*0.25*
Mean Absolute Permeability (mD)	*900*
Average Irreducible Water Saturation (-)	*0.19*
Net to Gross (-)	*0.7-1*

b. Geological Description

In figure 9 (Fig.9) is represented a stratigraphic representation of the Norne field, detailing its geological formations, depositional environments, and reservoir properties. The column spans the Lower to Middle Jurassic periods, specifically from the Pliensbachian to Callovian ages. It covers two major groups: the Båt Group (Tilje and Tofte formations) and the Fangst Group (Ile and Garn formations). Each formation is further subdivided into units (e.g., Tilje 1–4, Tofte 1–2), reflecting variations in depositional environments and reservoir characteristics. The depositional environments are represented using distinct color codes and patterns. Channelized sandstones (yellow with cross-hatching), shallow marine shoreface deposits (yellow with dots), lower shoreface to offshore transitions (green with horizontal lines), tidally influenced deposits (red with dots), bay deposits (brown with dots), and mouth bars (yellow with curved lines) are all depicted. Cemented horizons are shown in gray, while unconformities or sequence boundaries are marked by red wavy lines. Reservoir properties such as permeability, porosity, grain size, and thickness are summarized for each unit. Permeability ranges from 100 to 2500 mD in the Båt group formation and from 10 to 1000 mD in the Fangst group formation, indicating varying fluid flow capacities. Porosity averages between 18% and 25%, suggesting good hydrocarbon storage potential. Grain sizes range from very fine sandstones (0.062 mm) to fine sandstones (0.177 mm), consistent with high-quality reservoirs. The average thickness of individual units varies from 9 m to 35 m, contributing to the overall reservoir volume. Crucial observations include the Garn Formation's high permeability and porosity, making it an excellent gas reservoir, while the Tilje Formation exhibits more complex depositional environments, including bay deposits and lower shoreface transitions. This

stratigraphic column provides critical insights into the Norne field's reservoir heterogeneity, helping in understanding fluid flow dynamics and optimizing hydrocarbon recovery strategies.

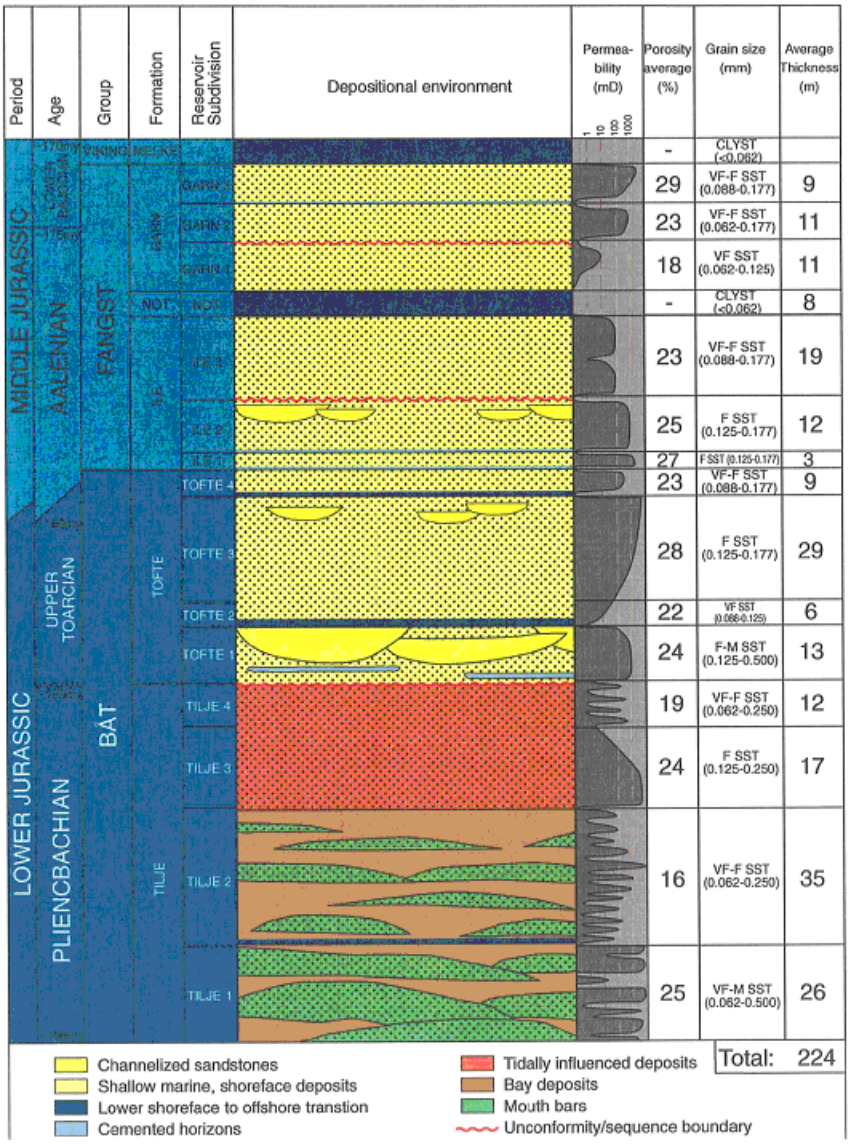

Figure 9:Stratigraphical sub-division of Norne Reservoir

c. *Model Description*

The figure below (Fig.10) generated using FloViz 2020.1 software, presents a three-dimensional static model of the Norne field reservoir, displaying the distribution of different fluid saturations. The visualization offers a comprehensive representation of the field's geological structure, using a color-coded scheme where red represents gas saturation, blue indicates water saturation, and green shows oil saturation. The model reveals a complex geological structure with a distinctive elongated shape, characterized by multiple zones of fluid contacts and varying saturations throughout the reservoir. The predominant red central region suggests a significant gas cap, surrounded by oil-bearing zones (green) and water-bearing sections (blue) at the flanks and lower portions of the structure.

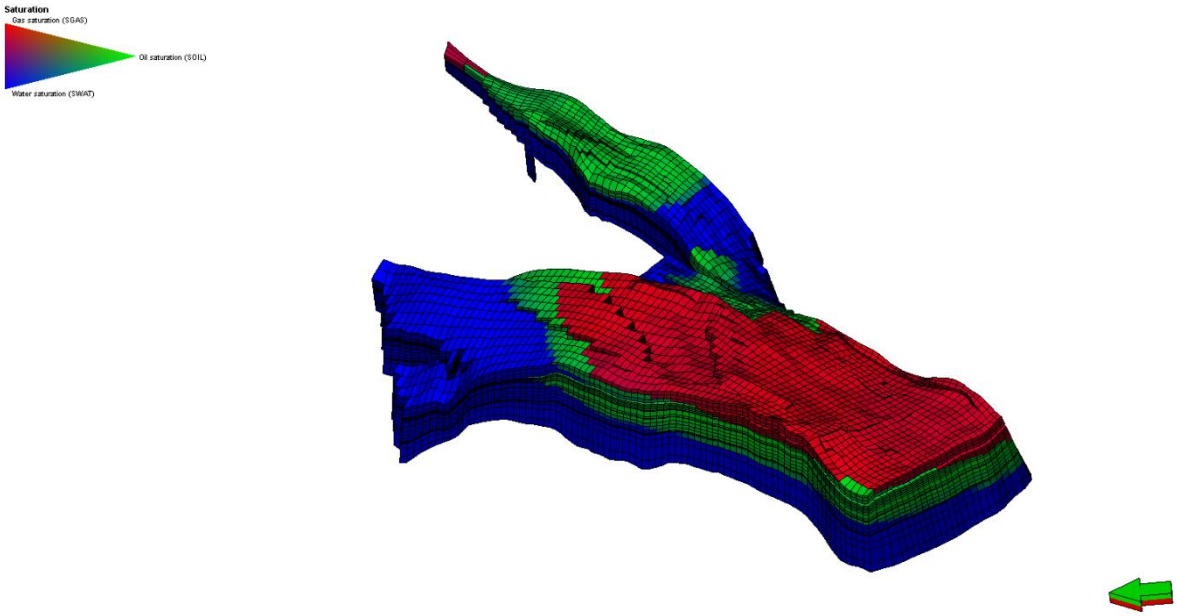

Figure 10: Static Model on FloViz Before Production

The Norne field is compartmentalized into four distinct segments: C, D, E, and G. Compartment C accounts for approximately 70% of the field's total production. The figure below (Fig.11), shows how the field compartments are distributed geographically, and the table (table 1) presents their top depth.

Table 2: Formations Top Depth

FORMATION TYPE	TOP DEPTH(M)
GARN	2578
ILE	2619
TOFTE	2668
TILJE	2720

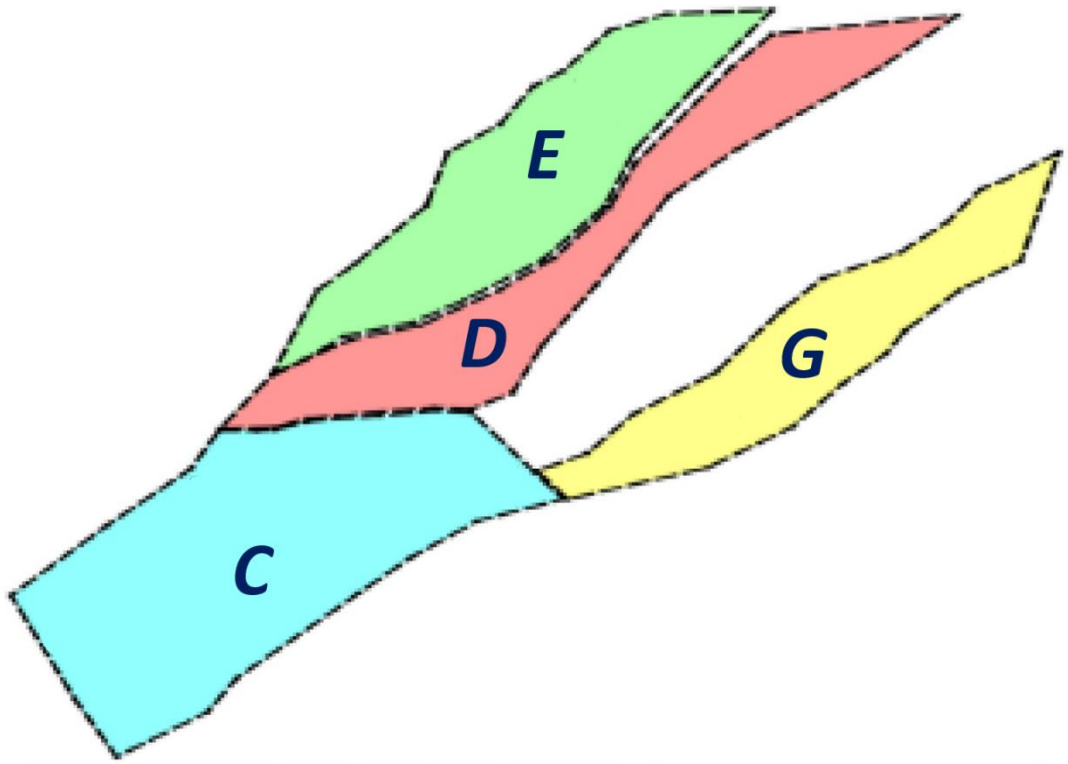

Figure 11: Norne Field Segments Locations

3. Dynamic Model

a. Reservoir Production and Pressure History

The Norne field's historical production and pressure trends offer valuable insights into how reservoirs deplete and how different production strategies affect pressure changes as the figure 12 (fig. 12) illustrates. This information is crucial when evaluating the field's potential for underground carbon storage (UCS). Typically, such fields undergo significant changes in oil, gas, and water production over time, as shown in cumulative production graphs (fig. 13, 14 and 15). Meanwhile, reservoir pressure declines due to hydrocarbon extraction and enhanced recovery techniques, which can be observed in pressure trend graphs.

In general, fields like Norne use a combination of primary and secondary recovery methods. Primary production relies on the natural pressure of the reservoir, while secondary methods, such as water injection, help maintain or increase pressure to extract more resources. Understanding these dynamics is essential for assessing the suitability of a field for carbon storage.

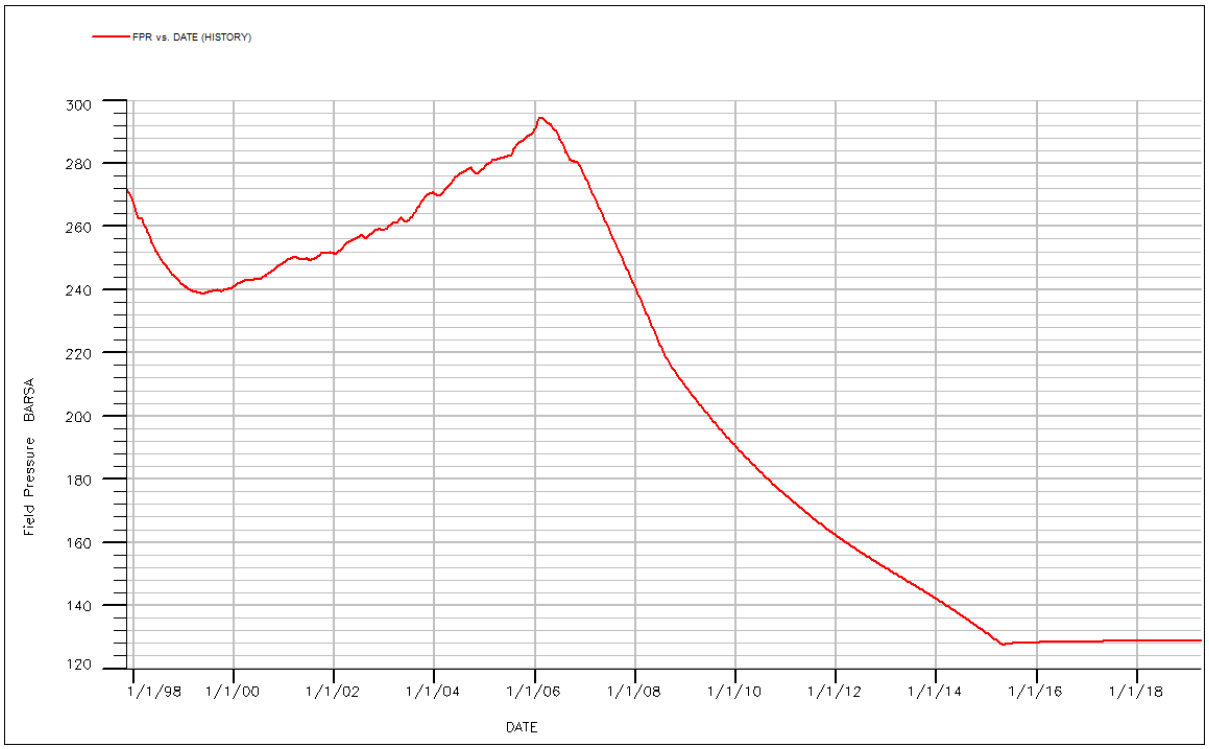

Figure 12: Field Pressure vs Time

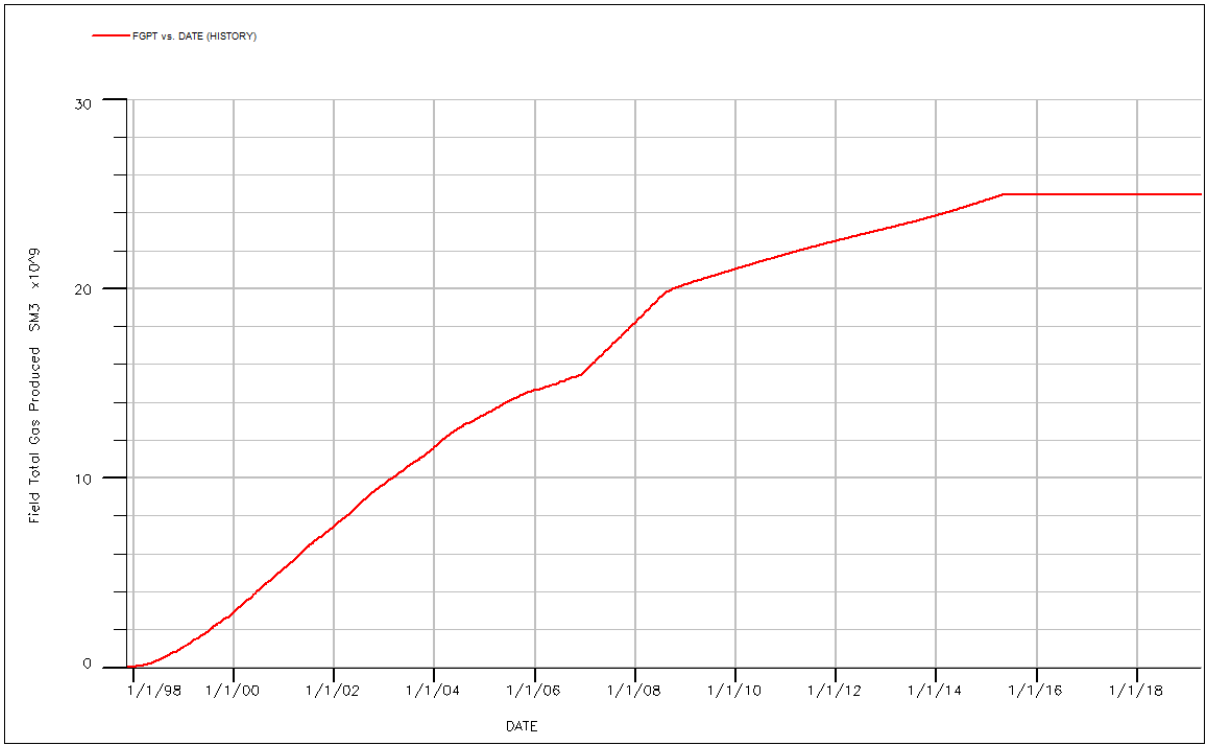

Figure 13: Field Cumulative Gas Production vs Time

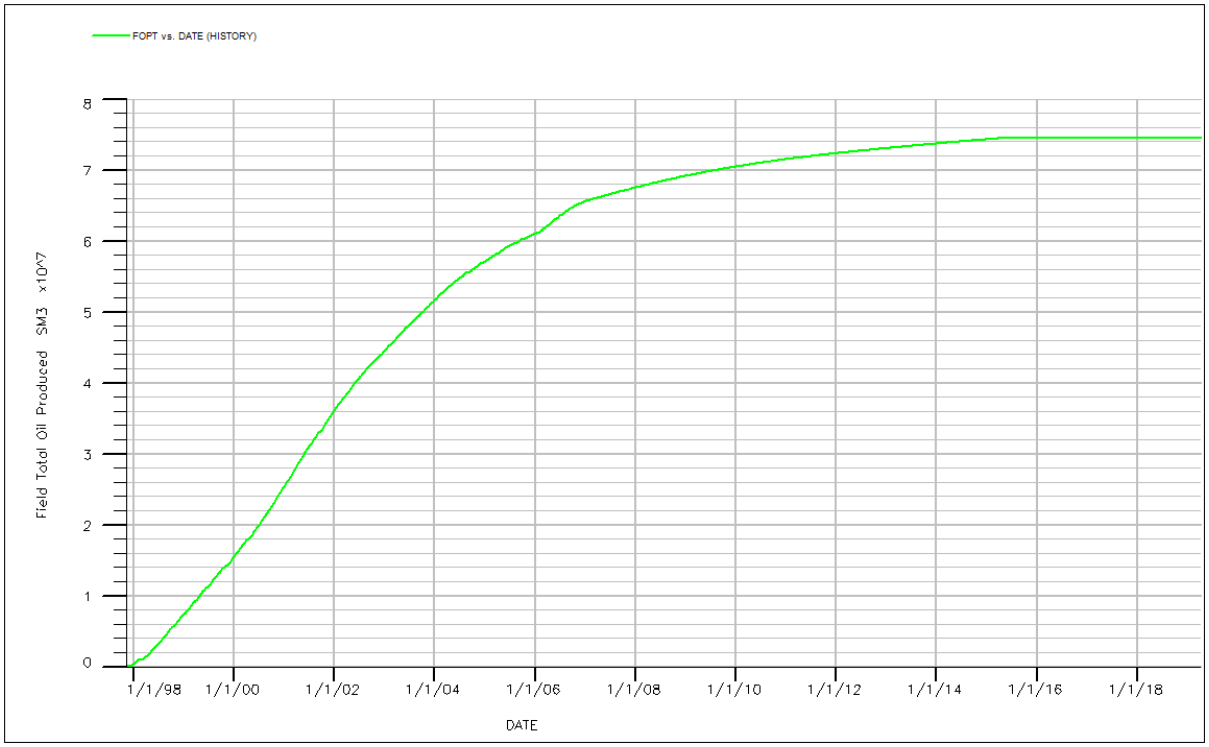

Figure 14: Field Cumulative Oil Production vs Time

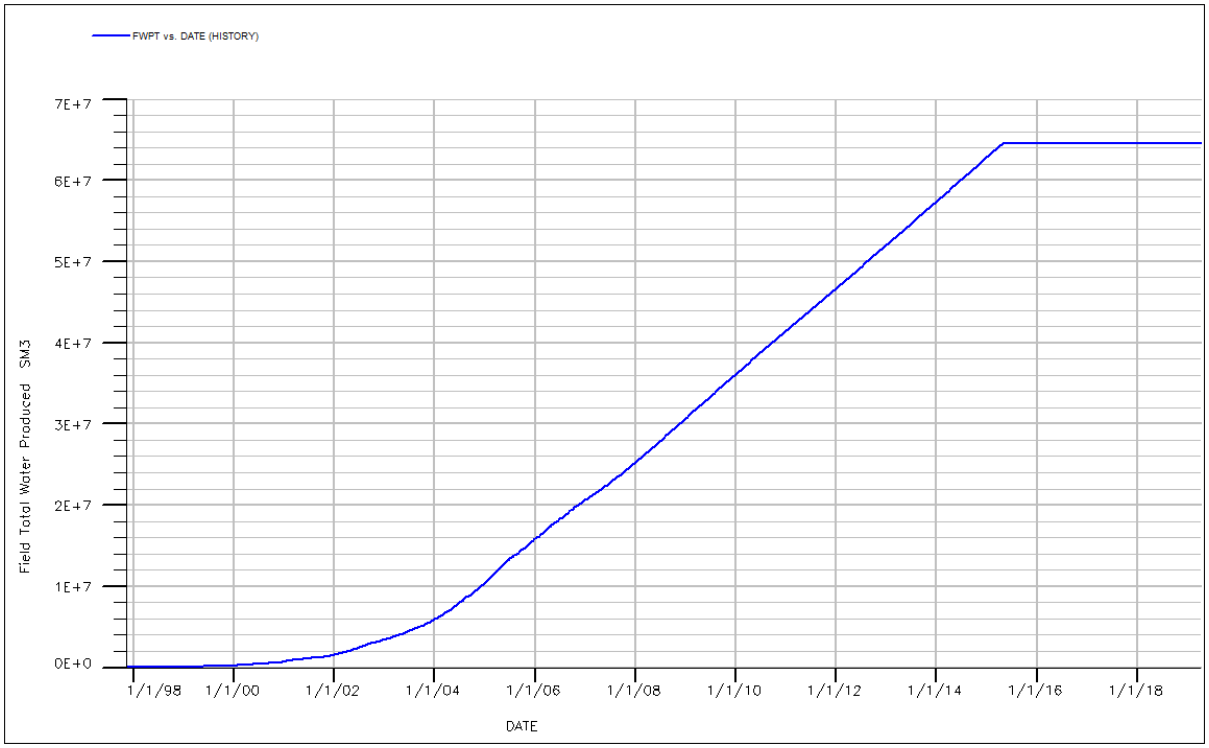

Figure 15: Field Cumulative Water Production vs Time

Initially, the field experienced a gradual decline in pressure due to hydrocarbon extraction, with gas cap expansion playing a key role in maintaining production rates. To counteract this decline, Water Alternating Gas (WAG) injection was employed from 1998 to 2005, successfully stabilizing reservoir pressure and improving the efficiency of hydrocarbon recovery.

Following the termination of WAG injection in 2006, the reservoir pressure began to decline gradually. This period saw oil production reach its peak and then decrease, while gas production increased significantly, marking a shift towards gas-dominated production. The sharp drop in reservoir pressure, from about 290 bars to 125 bars, was accompanied by a decrease in oil output and an increase in gas production. As the field approached depletion, water production also rose, reflecting higher water content in the extracted fluids. By 2015, when production ceased, the reservoir pressure had stabilized at around 120-130 bar.

The Norne field's development involved the drilling of 36 wells in total (fig. 16), comprising both production and injection wells. Over its operational period from 1997 to 2015, the field yielded substantial hydrocarbon resources. Cumulative production reached 70 million standard cubic meters of oil and 5 billion standard cubic meters of gas. These figures are significant when compared to the initial estimates of the field's resources. The original oil in place was assessed at approximately 160 million standard cubic meters, while the original gas in place was estimated at around 27 billion standard cubic meters.

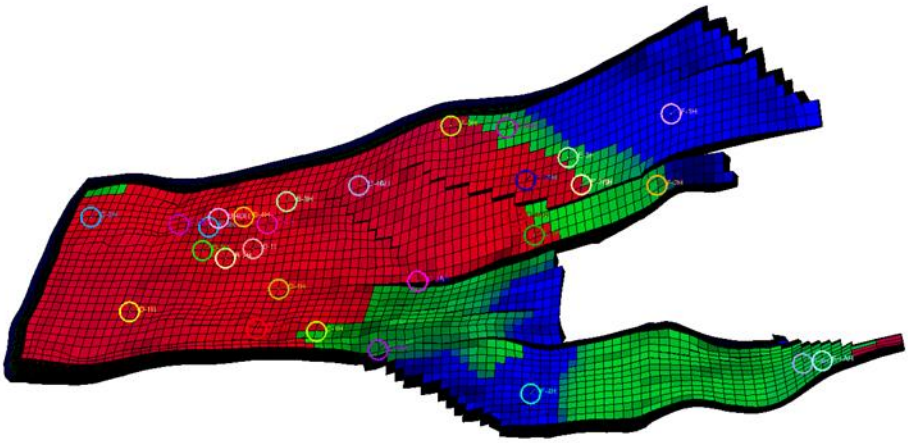

Figure 16: Norne Field's Wells Locations

The Norne field's depletion history suggests it could be well-suited for CO_2 storage. The stabilized pressure offers ample space for CO_2 injection, and the remaining gas cap provides a suitable medium for storage. The field's past experience with WAG injection demonstrates its ability to handle re-pressurization, as the figures 17 and 18 (fig. 17 and 18) show the total gas and water injected during this phase, which is beneficial for maintaining pressure during CO_2 storage. Additionally, the existing infrastructure, including multiple wells, can be adapted for CO_2 injection and monitoring. Overall, the field's capacity to manage pressure fluctuations and its existing infrastructure make it a promising site for CO_2 storage.

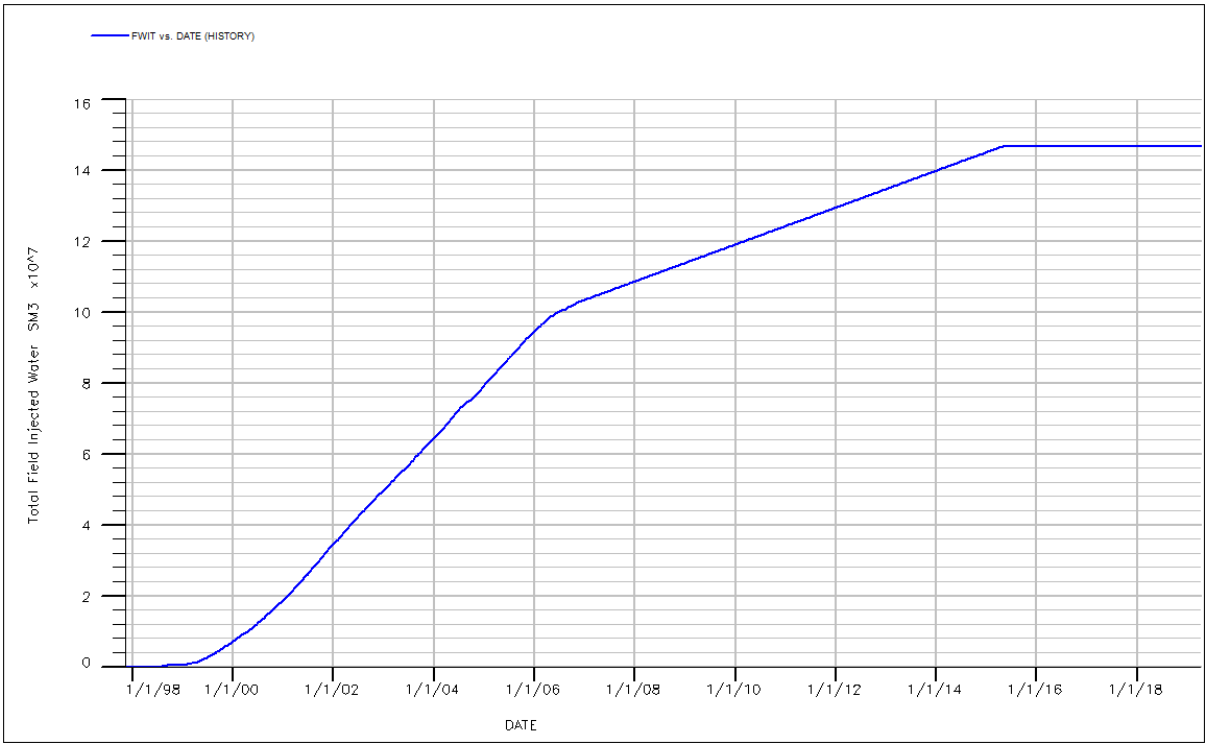

Figure 17: Total Field Injected Water

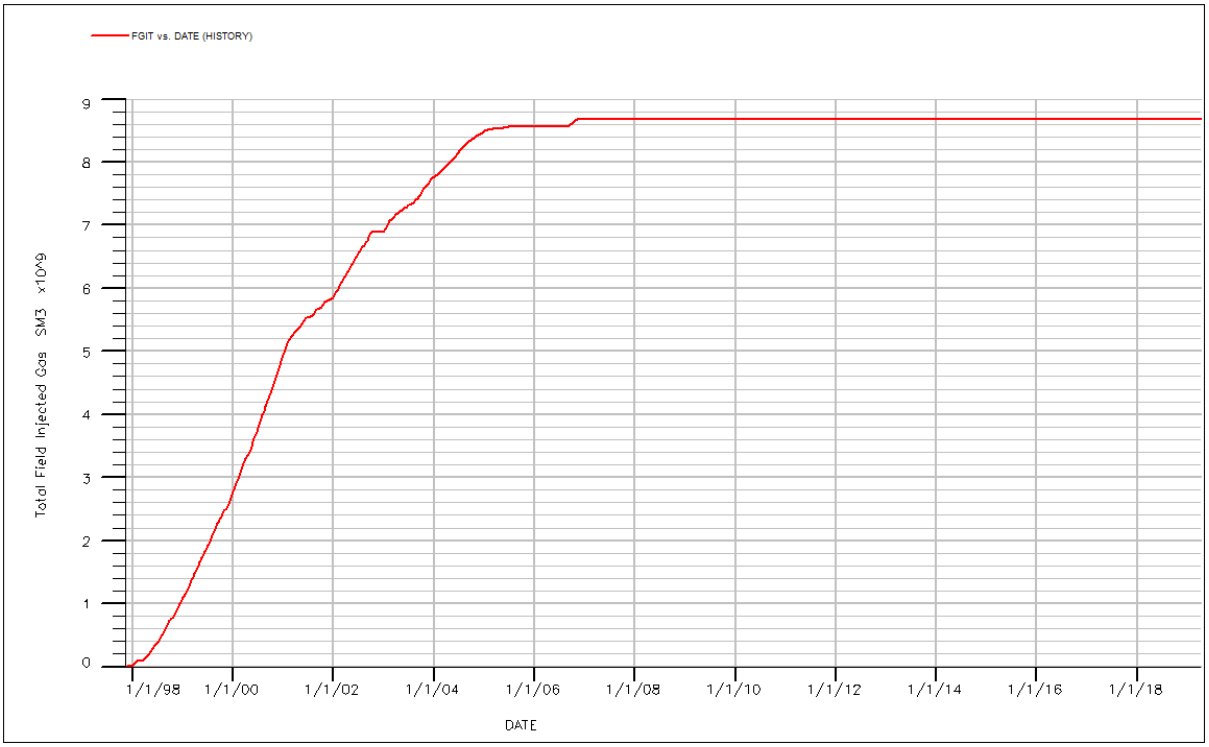

Figure 18: Total Field Injected Gas

Table 3: Reservoir HOIP and Production

	Production and Injection History	*Value*
Oil	OOIP	*160 million sm^3*
	Total oil production (1997-2015)	*75 million sm^3*
Gas	GOIP	*27 billion sm^3*
	Total gas production (1997-2015)	*25 billion sm^3*
	Total Field Injected Gas	*8.68 billion sm^3*
Water	Total Field Injected Water	*146 million sm^3*

b. *Forecast scenarios for CO_2 storage*

The dynamic simulation of CO_2 injection in the Norne reservoir was conducted using ECLIPSE 100, with visualization performed in FLOVIZ and Eclipse Office. Since the Norne field is a depleted hydrocarbon reservoir with a well-documented production and injection history, this study focuses on repurposing existing wells within the gas cap region for CO_2 injection and monitoring. This approach ensures a practical assessment of storage feasibility while minimizing the need for additional infrastructure. The primary objective is to evaluate how different injection strategies impact storage efficiency, pressure stability, and CO_2 retention while ensuring that reservoir conditions remain within safe operational limits. The study considers three different injection scenarios over a 15-year period from 2019 to 2034. In the base case, CO_2 is injected through a single well at a rate of 2×10^6 Sm^3/day. Case 1 involves injection into eight wells, same wells that were used historically and present in the gas cap, at 500,000 Sm^3/day, while Case 2 increases the injection rate to 750,000 Sm^3/day across the same

eight wells. Each scenario operates under the same constraints, with a maximum bottom-hole pressure (BHP) of 270 bars, corresponding to the initial gas cap pressure, to prevent excessive stress that could lead to fracturing or leakage risks.

The simulation is structured to evaluate CO_2 migration, pressure evolution, and retention within the reservoir, with a particular focus on structural trapping as the primary storage mechanism. An initial stabilization period is implemented before continuous injection begins. Over the 15-year period, key performance indicators such as gas in place (GIP), regional pressure variations, and CO_2 distribution are analyzed. GIP trends provide insight into storage capacity and efficiency, while pressure evolution ensures operational safety throughout the injection phase. The distribution of CO_2 is assessed to understand its mobility, retention losses, and overall containment stability under different injection scenarios. By comparing the results across all three cases, this study aims to determine the most effective injection strategy for maximizing storage efficiency while maintaining reservoir integrity and minimizing potential risks.

The injection strategies in this study are designed to evaluate the effectiveness of different well configurations and injection rates in maximizing CO_2 storage while ensuring reservoir stability. By considering various injection scenarios, the study aims to assess the impact on pressure distribution, storage efficiency, and CO_2 retention within the Norne reservoir. The following table recaps the 3 cases performed.

Table 4: Cases Conditions

Case	*Well Configuration (Number of Wells)*	*Injection Rate per Well (sm^3/day)*	*Total Injection Rate(sm^3/day)*	*Mass CO2 Injection (million tons)*
Base Case	*1*	*$2*10^6$*	*$2*10^6$*	*20.38*
Case 1	*8*	*$0.5*10^6$*	*$4*10^6$*	*40.76*
Case 2	*8*	*$0.75*10^6$*	*$6*10^6$*	*61.14*

c. *Results and Discussion*

The graph below illustrates the relationship between field pressure response (FPR) and injection rate over time for the three CO_2 injection scenarios analyzed in this study. The left y-axis represents the field pressure in barsa, while the right y-axis corresponds to the injection rate in standard cubic meters per day (Sm^3/day). The time scale on the x-axis spans multiple years, from the early stages of production until the end of the injection of CO_2, allowing us to observe both the transient and long-term behavior of the reservoir under different injection conditions. By analyzing the distinct trends in pressure buildup and injection stabilization, we can correlate these results with the three cases and compare their effectiveness in maximizing CO_2 storage while ensuring reservoir stability.

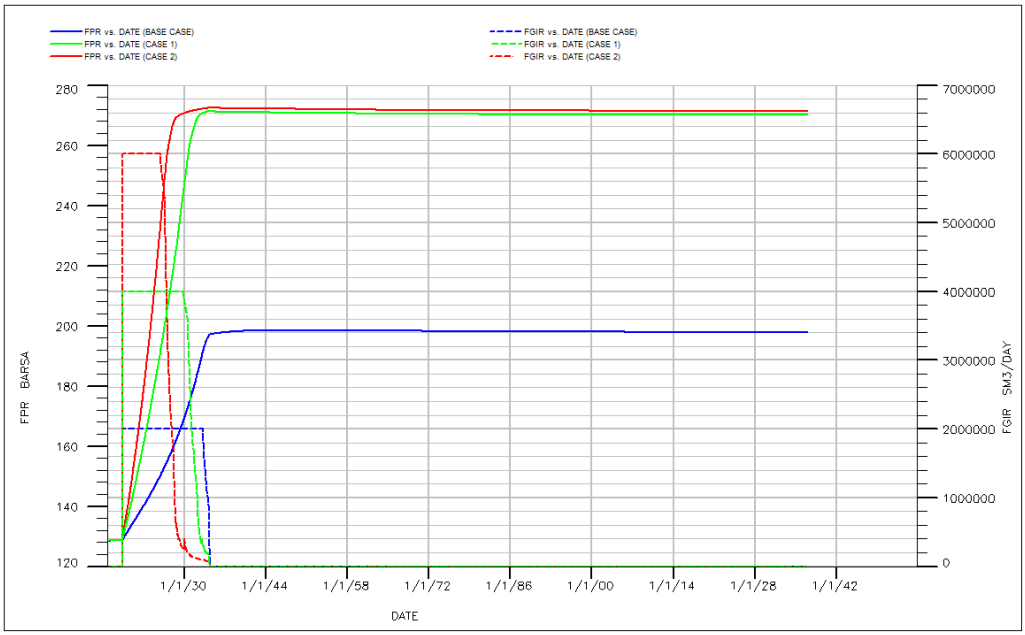

Figure 19: Field Pressure and Injection Rate vs Time (all cases)

The injection rate curves display three distinct plateaus, each corresponding to one of the studied cases. The base case, which involves a single injection well operating at 2,000,000 sm^3/day, exhibits the lowest injection plateau. Over time, this case leads to a moderate increase in reservoir pressure, as observed in the pressure response curve. Since the CO_2 is injected through a single well, the pressure is concentrated in one region, potentially limiting the reservoir's overall storage efficiency. However, the pressure buildup remains relatively controlled, indicating a lower risk of exceeding reservoir pressure limits.

In case 1, the injection rate is doubled to 4,000,000 Sm^3/day by distributing the injection across eight wells. This configuration results in a higher injection plateau compared to the Base Case, as seen in the graph. The pressure response curve shows a more gradual and distributed increase, suggesting improved reservoir stability. The multi-well setup helps distribute the

injected CO_2 more evenly, reducing the likelihood of localized pressure spikes. As a result, case 1 offers a balanced approach, allowing for increased storage without significant overpressure concerns.

Case 2, which features the highest injection rate at 6,000,000 Sm^3/day, reaches the highest injection plateau. The pressure response in this scenario demonstrates a substantial increase compared to the other cases, reflecting the challenge of accommodating such a large volume of CO_2 within the reservoir. While this case maximizes CO_2 storage, the pressure buildup could exceed safe operating limits, increasing the risk of cap rock failure or CO_2 leakage. The pressure stabilization seen in the later stages of the graph suggests that the reservoir is absorbing the CO_2, but the high-pressure levels indicate the need for careful pressure management strategies.

Comparing the three cases, it is evident that Case 2 offers the highest injection volume while reaching the initial pressure of the reservoir. The base case, while safer in terms of pressure management, underutilizes the reservoir's capacity and may not be the most efficient approach for long-term CO_2 sequestration. On the other hand, Case 1, despite injecting a decent volume of CO_2, does not reach the reservoir's full storage potential. Therefore, Case 2 emerges as the most practical solution, allowing for higher injection volumes while keeping pressure levels within a manageable range.

Table 5: Cases Comparison

Case	*Injection Rate ($x10^6 Sm^3/day$)*	*Reservoir Storage Utilization*	*Pressure Management*	*CO2, Storage Efficiency*	*Overall Assessment*
Base Case	2	Low	Safe, minimal pressure buildup	Low, underutilizes reservoir	Safe but inefficient
Case 1	4	Moderate to High	Balanced, controlled pressure increase	Moderate efficiency, room for improvement	Practical and balanced, yet not sufficient
Case 2	6	High	High pressure, some risk of exceeding limits	Optimal balance of storage and stability	Reaching full storage potential.

The figures provided (Fig. 20, 21 and 22) below illustrate the distribution of CO_2 saturation within the gas cap of a reservoir for three different simulation scenarios.

In the base case (Fig. 20), CO_2 appears to be concentrated in the lower section of the gas cap structure, indicated by the yellow and green areas, with limited migration into the upper reaches of the structure, which are predominantly blue/purple.

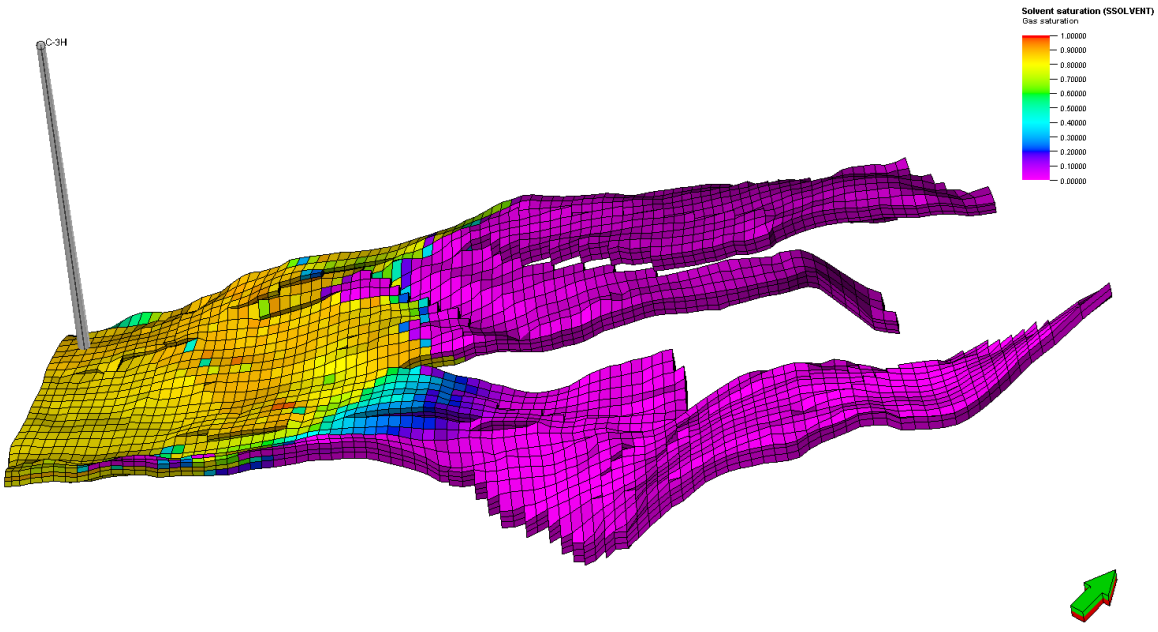

Figure 20: Base Case, CO_2 distribution

Meanwhile, in case 1 (Fig. 21) shows a broader distribution of CO_2 saturation compared to the first. While the highest concentrations remain in the central section, the CO_2 has migrated further upwards within the gas cap structure, as evidenced by the more extensive yellow and green areas.

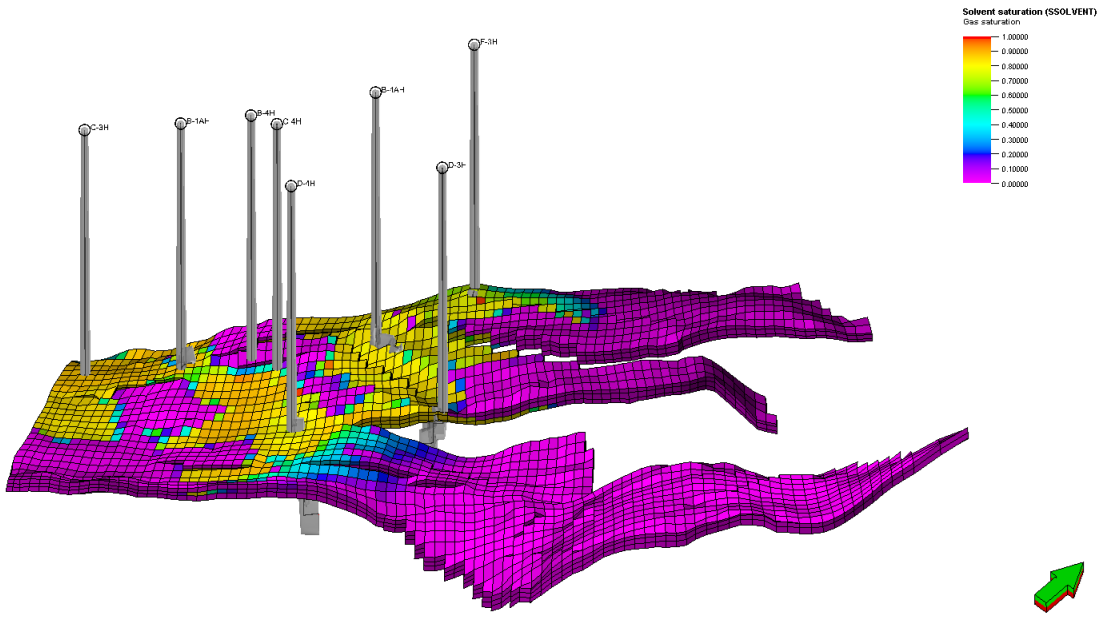

Figure 21: Case 1, CO_2 distribution

Whereas, in case 2 (Fig. 22) shows a continued trend of CO_2 migration within the gas cap. The CO_2 saturation is even more widespread, covering a larger portion of the structure compared to the previous two cases.

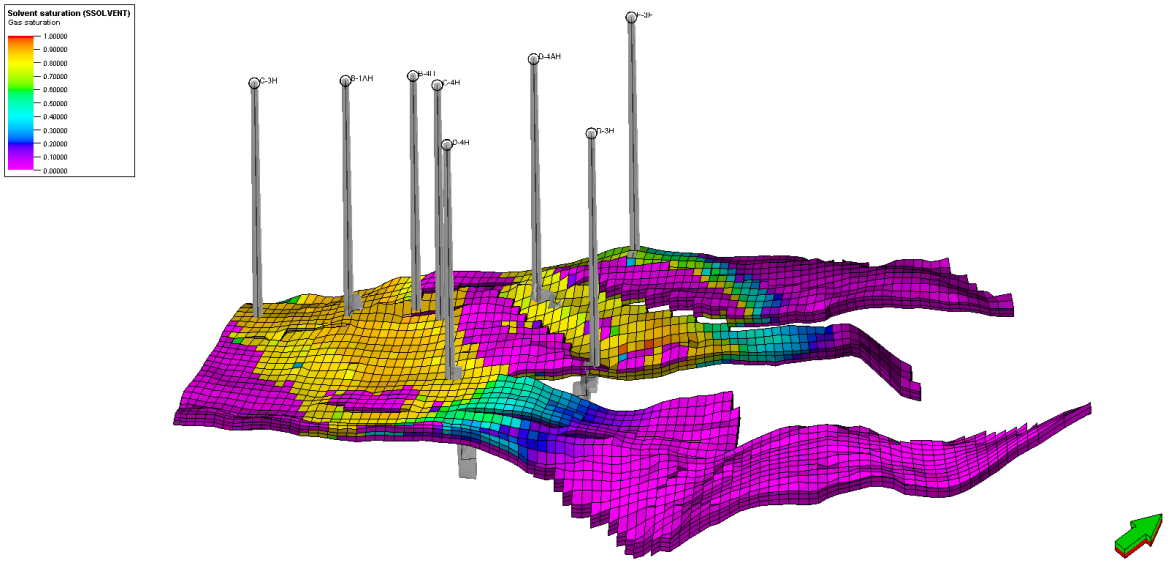

Figure 22: CO_2 Distribution, Case 2

IV. Conclusion and Future Works

This study successfully reconstructed an existing static model and utilized dynamic modeling to assess the feasibility of repurposing the Norne Field, a depleted hydrocarbon reservoir, for CO_2 sequestration. The static model, built using data from the OPM initiative and visualized with FloViz, provided a comprehensive 3D representation of the reservoir's geological structure, compartmentalization into segments C, D, E, and G, and key petrophysical properties like porosity (averaging 25%) and permeability (averaging 900 mD). Dynamic simulations, conducted with ECLIPSE® 100 of Schlumberger, evaluated three injection strategies over a 15-year period, focusing on gas cap injection through existing wells to minimize infrastructure requirements. The base case, involving injection through a single well at 2 million sm^3/day, resulted in a total CO_2 injection of 20.38 million tons but showed limited distribution within the gas cap. Case 1, utilizing eight wells at 0.5 million sm^3/day per well, achieved a total injection of 40.76 million tons, providing a moderate balance between storage volume and pressure management. Case 2, injecting through eight wells at 0.75 million sm^3/day per well, maximized CO_2 injection to 61.14 million tons using the full potential of the reservoir within safe pressure limits. Comparative analysis indicated that Case 2 offers the most practical approach, balancing storage efficiency and reservoir stability. The study underscores the importance of comprehensive reservoir modeling in optimizing injection strategies and ensuring safe, efficient geological storage of CO_2 in depleted hydrocarbon reservoirs.

Future work should employ compositional simulators like ECLIPSE 300 enabling a more detailed analysis of phase behavior and geochemical interactions. This will provide insights into long-term storage security and potential enhanced hydrocarbon recovery. Ultimately, this

research supports the viability of CCUS technology in mature hydrocarbon reservoirs for sustainable energy practices.

References:

1. Metz, B., Davidson, O., de Coninck, H. C., Loos, M., & Meyer, L. A. (Eds.). (2005). *IPCC special report on carbon dioxide capture and storage*. Cambridge University Press.
2. Pires, A., Martinho, G., & Chang, N.-B. (2011). Solid waste management in European countries: A review of systems analysis techniques. *Journal of Environmental Management, 92*(4), 1033–1050. https://doi.org/10.1016/j.jenvman.2010.11.024
3. Benson, S. M., & Cole, D. R. (2008). CO2 sequestration in deep sedimentary formations. *Elements, 4*(5), 325–331. https://doi.org/10.2113/gselements.4.5.325
4. Lackner, K. S., Brennan, S., Matter, J. M., Park, A. H. A., Wright, A., & Van Der Zwaan, B. (2012). The urgency of the development of CO2 capture from ambient air. *Proceedings of the National Academy of Sciences, 109*(33), 13156–13162. https://doi.org/10.1073/pnas.1108765109
5. Bachu, S. (2008). CO_2 storage in geological media: Role, means, status and barriers to deployment. *International Journal of Greenhouse Gas Control, 2*(2), 234–246. https://doi.org/10.1016/j.ijggc.2007.12.001
6. Ringrose, P. S., & Meckel, T. A. (2019). Maturing global CO2 storage resources on offshore continental margins to achieve 2DS emissions reductions. *Scientific Reports, 9*(1), Article 17944. https://doi.org/10.1038/s41598-019-54363-z
7. Michael, K., Golab, A., Shulakova, V., Ennis-King, J., Allinson, G., Sharma, S., & Aiken, T. (2010). Geological storage of CO_2 in saline aquifers—A review of the experience from existing storage operations. *International Journal of Greenhouse Gas Control, 4*(4), 659–667. https://doi.org/10.1016/j.ijggc.2009.12.011

8. Gale, J., & Davidson, O. (2004). Transmission of CO_2—Safety and economic considerations. *Energy,29*(9–10),1319–1328. https://doi.org/10.1016/j.energy.2004.03.090

9. Hosa, A., Esentiawati, R., Harper, P., McDermott, C., & Smithson, K. (2011). Geological storage of carbon dioxide: A review and comparison of its potential environmental risks with those of other storage options. *International Journal of Greenhouse Gas Control*, *5*(6), 1003–1015. https://doi.org/10.1016/j.ijggc.2011.08.014

10. Bickle, M., Chadwick, A., Huppert, H., Hallworth, M., & Lyle, S. (2007). Modelling carbon dioxide accumulation at Sleipner: Implications for underground carbon storage. *Earth and Planetary Science Letters*, *255*(1–2), 164–176. https://doi.org/10.1016/j.epsl.2006.12.013

11. Bachu, S., & Adams J.J. (2003). Sequestration of CO_2 in geological media in response to climate change: Capacity of deep saline aquifers to sequester CO_2 in solution. *Energy Conversion and Management*, *44*(20), 3151–3175. https://doi.org/10.1016/S0196-8904(03)00101-8

12. Bachu, S. (2015). Review of CO_2 storage efficiency in deep saline aquifers. *International Journal of Greenhouse Gas Control, 40*, 188–202. https://doi.org/10.1016/j.ijggc.2015.01.007

13. Solomon, S. D. (2006). *Carbon dioxide storage: Geological security and environmental issues – Case study on the Sleipner Gas Field in Norway*. The Bellona Foundation. https://bellona.org/assets/sites/3/2015/06/fil_Paper_Solomon_-_CO2_Storage.pdf

14. Hermanrud, C., Andresen, T., Eiken, O., Hansen, H., Janbu, A., Lippard, J., Bolås, H., Simmenes, T. H., Teige, G., & Østmo, S. (2009). Storage of CO_2 in saline aquifers: Lessons

learned from 10 years of injection into the Utsira Formation in the Sleipner area. *Energy Procedia, 1*(1), 1997–2004. https://doi.org/10.1016/j.egypro.2009.01.260

15. Huppert, H. E., & Neufeld, J. A. (2014). The fluid mechanics of carbon dioxide sequestration. *Annual Review of Fluid Mechanics, 46*(1), 255–272. https://doi.org/10.1146/annurev-fluid-011212-140627
16. Juanes, R., MacMinn, C. W., & Szulczewski, M. L. (2010). The footprint of the CO_2 plume during carbon dioxide storage in saline aquifers: Storage efficiency for capillary trapping at the basin scale. *Transport in Porous Media, 82*(1), 19–30. https://doi.org/10.1007/s11242-009-9420-3
17. Kampman, N., Bickle, M., Wigley, M., & Dubacq, B. (2014). Fluid flow and CO_2-fluid-mineral interactions during CO_2-storage in sedimentary basins. *Chemical Geology, 369*, 22–50. https://doi.org/10.1016/j.chemgeo.2013.11.012
18. Matter, J. M., Stute, M., Snaebjornsdottir, S. O., Oelkers, E. H., Gislason, S. R., Aradottir, E. S., & Sigfusson, B. (2016). Rapid carbon mineralization for permanent disposal of anthropogenic carbon dioxide emissions. *Science, 352*(6291), 1312–1314. https://doi.org/10.1126/science.aad8132
19. Raza, A., Gholami, R., Rabiei, M., Rasouli, V., Rezaee, R., & Fakhari, N. (2019). Impact of geochemical and geomechanical changes on CO2 sequestration potential in sandstone and limestone aquifers. *Greenhouse Gases Science and Technology*, *9*(5), 905–923. https://doi.org/10.1002/ghg.1907
20. UNILAB Srl. (2019). *What happens to fluid properties near the critical point?* https://www.unilab.eu/articles/fluid-properties-near-critical-point/

21. Ramazanova, A., & Abdulagatov, I. (2021). Thermal conductivity of supercritical CO2-saturated coal. International Journal of Thermophysics, 42(1), Article 10. https://doi.org/10.1007/s10765-020-02756-y

22. Ouyang, L. B. (2011). New correlations for predicting the density and viscosity of supercritical carbon dioxide under conditions expected in carbon capture and sequestration operations. The Open Petroleum Engineering Journal, 4, 13-21. https://doi.org/10.2174/1874834101104010013

23. Vesely, L., Kancherla, R., Vasu, S., Kapat, J., Dostál, V., & Martin, S. (2018). Effect of impurities on compressor and cooler performances in supercritical CO2 cycles. Journal of Energy Resources Technology, 141. https://doi.org/10.1115/1.4040581

24. McBride-Wright, M., Maitland, G. C., & Trusler, J. P. M. (2015). Viscosity and density of aqueous solutions of carbon dioxide at temperatures from (274 to 449) K and at pressures up to 100 MPa. Journal of Chemical & Engineering Data, 60(1), 171-180. https://doi.org/10.1021/je5009125

25. Fenghour, A., Wakeham, W. A., & Vesovic, V. (1998). The viscosity of carbon dioxide. *Journal of Physical and Chemical Reference Data, 27*(1), 31–44. https://doi.org/10.1063/1.556013

26. Laesecke, A., & Muzny, C. D. (2017). Reference correlation for the viscosity of carbon dioxide. Journal of Physical and Chemical Reference Data, 46(1), Article 013107. https://doi.org/10.1063/1.4977429

27. Adisoemarta, P., Frailey, S. M., & Lawal, A. S. (2004). *Measurement of Z-factors for carbon dioxide sequestration*. Proceedings of the AIChE Annual Meeting. from https://skoge.folk.ntnu.no/prost/proceedings/aiche-2004/pdffiles/papers/167bc.pdf

28. Elsharkawy, A. M., & Elsharkawy, L.A. (2024). *Predicting the compressibility factor of natural gases containing various amounts of CO_2 at high temperatures and pressures*. *Journal of*

Petroleum and Gas Engineering. from https://academicjournals.org/journal/JPGE/article-full-text-pdf/A4C994063491

29. MDPI Energies Journal. (2023). *An improved correlation of compressibility factor prediction of variable CO_2-content condensate gases*. *Energies, 16*(1), 105. https://doi.org/10.3390/en16010105

30. Turkson, J. N., Muhammad, Ingebret Fjelde, Sokama-Neuyam, Y. A., Darkwah-Owusu, V., & Bennet Nii Tackie-Otoo. (2024). *Harnessing Ensemble Learning Techniques for Accurate Interfacial Tension Estimation in Aqueous CO2 Systems*. https://doi.org/10.2118/219176-ms

31. Johny Mouallem, Raza, A., Mahmoud, M., & Arif, M. (2023). Critical Review of Interfacial Tension of CO2-brine Systems: Implications for CO2 Storage. *Day 2 Wed, March 23, 2022*. https://doi.org/10.2118/214175-ms

32. Ahmed, Paker, D. M., Birol Dindoruk, Drylie, S., & Gautam, S. (2024). Quantification of the Effect of CO2 Storage on CO2-Brine Relative Permeability in Sandstone Reservoirs: An Experimental Study. *SPE Annual Technical Conference and Exhibition*, *462*. https://doi.org/10.2118/220974-ms

33. Mukherjee, S., & Johns, R. T. (2024). Relative Permeability Modeling for CO2 Storage Using Physically Constrained Artificial Neural Networks. *SPE Improved Oil Recovery Conference*. https://doi.org/10.2118/218160-ms

34. Chu, B., Feng, G., Zhang, Y., Qi, S., Li, P., & Huang, T. (2023). Residual Saturation Effects on CO2 Migration and Caprock Sealing: A Study of Permeability and Capillary Pressure Models. *Water*, *15*(18), 3316–3316. https://doi.org/10.3390/w15183316

35. Heath, J. E., Dewers, T. A., McPherson, B. J. O. L., Nemer, M. B., & Kotula, P. G. (2012). Pore-lining phases and capillary breakthrough pressure of mudstone caprocks: Sealing efficiency of geologic CO2 storage sites. *International Journal of Greenhouse Gas Control*, *11*, 204–220. https://doi.org/10.1016/j.ijggc.2012.08.001

36. Amer Alanazi, Ali, M., Mahmoud Mowafi, Saleh Bawazeer, Kaidar, Z. K., & Hussein Hoteit. (2023). Capillary-Sealing Efficiency of Mica-Proxy Caprock for CO2/H2 Geologic Storage in the Presence of Organic Acids and Nanofluids. *SPE Journal*, *28*(06), 3308–3323. https://doi.org/10.2118/217471-pa

37. Kou, Z., Wang, H., Alvarado, V., Nye, C., Bagdonas, D. A., McLaughlin, J. L., & Quillinan, S. (2022). *Effects of Carbonic Acid-Rock Interactions on CO2/Brine Multiphase Flow Properties in the Upper Minnelusa Sandstones*. 1–14. https://doi.org/10.2118/212272-pa

38. Wan, Y., Jia, C., Zhao, W., Jiang, L., & Chen, Z. (2023). Micro-Scale Lattice Boltzmann Simulation of Two-Phase CO2–Brine Flow in a Tighter REV Extracted from a Permeable Sandstone Core: Implications for CO2 Storage Efficiency. *Energies*, *16*(3), 1547–1547. https://doi.org/10.3390/en16031547

39. Tatar, A., Shokrollahi, A., Lee, M., Kashiwao, T., & Bahadori, A. (2015). Prediction of supercritical CO2/brine relative permeability in sedimentary basins during carbon dioxide sequestration. Greenhouse Gases: Science and Technology, 5(6), 756–771. https://doi.org/10.1002/ghg.1524

40. Jia, W., McPherson, B., Pan, F., Dai, Z., Moodie, N., & Xiao, T. (2018). Impact of Three-Phase Relative Permeability and Hysteresis Models on Forecasts of Storage Associated With CO2-EOR. *Water Resources Research*, *54*(2), 1109–1126. https://doi.org/10.1002/2017wr021273

41. Delshad, M., Kong, X., & Wheeler, M. F. (2011). On Interplay of Capillary, Gravity, and Viscous Forces on Brine/CO2 Relative Permeability in a Compositional and Parallel Simulation Framework. *All Days*. https://doi.org/10.2118/142146-ms

42. Kaveh, N. S. (2014). *Interfacial Interactions and Wettability Evaluation of Rock Surfaces for CO2 Storage*. https://doi.org/10.4233/uuid:5c1896f1-599f-4eb6-ae00-f2e690097a6e

43. Tariq, Z., Ali, M., Yan, B., Sun, S., Khan, M., Nurudeen Yekeen, & Hussein Hoteit. (2023). *Data-Driven Machine Learning Modeling of Mineral/CO2/Brine Wettability Prediction: Implications for CO2 Geo-Storage*. https://doi.org/10.2118/213346-ms

44. Xu, R., Yan, T., Han, X., Qu, J., & Feng, J. (2023). Mass Transfer Analysis of CO2-Water-Rock Geochemical Reactions in Reservoirs. *Energies*, *16*(16), 5862–5862. https://doi.org/10.3390/en16165862

45. Aldin, J., Tehrani, D. M., & Bazvand, M. (2022). Investigation of the effects of carbon dioxide injection on the rock and fluid intraction in high permeable sandstone reserviors. *Petroleum Science and Technology*, *41*(4), 387–405. https://doi.org/10.1080/10916466.2022.2060257

46. OPM. (2019). *opm-data/norne at master · OPM/opm-data*. GitHub. https://github.com/OPM/opm-data/tree/master/norne

47. *Field: NORNE - Norwegianpetroleum.no*. (2024, February 10). Norwegianpetroleum.no. https://www.norskpetroleum.no/en/facts/field/norne/